

# Annual Review of Fluid Mechanics The Fluid Mechanics of Deep-Sea Mining

## Thomas Peacock and Raphael Ouillon

Department of Mechanical Engineering, Massachusetts Institute of Technology, Cambridge, Massachusetts, USA; email: tomp@mit.edu

Annu. Rev. Fluid Mech. 2023. 55:403-30

First published as a Review in Advance on October 13, 2022

The *Annual Review of Fluid Mechanics* is online at fluid.annualreviews.org

https://doi.org/10.1146/annurev-fluid-031822-010257

Copyright © 2023 by the author(s). This work is licensed under a Creative Commons Attribution 4.0 International License, which permits unrestricted use, distribution, and reproduction in any medium, provided the original author and source are credited. See credit lines of images or other third-party material in this article for license information.

## ANNUAL CONNECT

#### www.annualreviews.org

- · Download figures
- · Navigate cited references
- Keyword search
- · Explore related articles
- · Share via email or social media

#### **Keywords**

sediment transport, sediment plumes, physical oceanography, turbidity currents, settling, flocculation

#### **Abstract**

Fluid mechanics lies at the heart of many of the physical processes associated with the nascent deep-sea mining industry. The evolution and fate of sediment plumes that would be produced by seabed mining activities, which are central to the assessment of the environmental impact, are entirely determined by transport processes. These processes, which include advection, turbulent mixing, buoyancy, differential particle settling, and flocculation, operate at a multitude of spatiotemporal scales. A combination of historical and recent efforts that combine theory, numerical modeling, laboratory experiments, and field trials has yielded significant progress, including assessing the role of environmental and operational parameters in setting the extent of sediment plumes, but more fundamental and applied fluid mechanics research is needed before models can accurately predict commercial-scale scenarios. Furthermore, fluid mechanics underpins the design and operation of proposed mining technologies, for which there are currently no established best practices.



#### Polymetallic nodule: a mineral concretion that forms at depths of around 5,000 m, lying partially buried in the seabed

#### Seafloor massive sulfide (SMS):

a deposit in the vicinity systems, along tectonic

deposit that forms over



Deep-sea mining is a new frontier in mineral extraction that is being actively pursued on the global stage, with potentially profound environmental and societal implications (Peacock & Alford 2018). It involves the recovery of rich and sometimes diverse mineral ores from the deep ocean, at depths ranging from around 1,000 m down to 6,000 m. In some cases, estimated resources of critical mineral deposits (e.g., nickel and cobalt) in parts of the abyssal ocean, most notably the Clarion-Clipperton Zone (CCZ) of the Pacific Ocean, exceed global land-based reserves severalfold (Hein et al. 2020). Proposed operations would take place in the deep ocean environment, and as such, fluid mechanics and transport phenomena play pivotal roles in understanding and modeling the relevant physics. This article surveys the current state of fluid mechanics knowledge in this area and identifies principal knowledge gaps.

Three different types of resources are being actively considered for extraction: polymetallic nodules, seafloor massive sulfides (SMSs), and cobalt crusts (Sharma 2017) (see Supplemental Figure 1). An artist's rendition of the associated deep-sea mining operations is presented in Figure 1. In all three cases, an operational vehicle or a combination of vehicles obtains the mineral ore, which is then raised to the surface via a vertical transport system. At the ocean surface, an operational vessel handles the mineral ore and may perform some preliminary preparation of it before shipment to a land-based processing facility, and in some cases there is a return water discharge into the ocean. One of the main differences between the three types of mining is the nature of the mineral gathering activity. In the case of polymetallic nodules, which are centimeter-scale concretions that lie partially buried in the seabed at depths of around 5,000 m, a collector vehicle system seeks to pick up the nodules from the abyssal plain while minimally disturbing and resuspending the upper layer of sediment in which they reside. In the case of SMS deposits, which exist around hydrothermal vents, a more direct form of mining is required to remove overburden and retrieve buried ores. For cobalt crusts, which are centimeter-thick crusts that form on the flanks of seamounts, the machinery must operate on the slopes of the seamount and be able to remove the desired crust.

A critical concern surrounding deep-sea mining is the potential impact of the associated sediment plumes on the biodiversity and ecosystem function of the deep ocean (Smith et al. 2020, Jones et al. 2021, Weaver et al. 2022). Since the sediment can be very fine, and thus the settling velocities very low, ocean currents have the ability to transport the sediment substantial distances, potentially causing indirect impact at faraway locations. While deep-ocean ecology is beyond the scope of this article, the question of the scale of the sediment plumes that will be generated and transported away from mining sites by background ocean currents, which is central to environmental impact assessment, is wholly underpinned by fundamental fluid mechanics and transport phenomena. Any sediment plumes generated by mining activities in the ocean have the potential to initially evolve under the effect of buoyancy while interacting with the background environment, before ultimately being passively transported by the background ocean current, and are subject to processes such as advection, turbulent mixing, and differential settling. This all contributes to the evolution of plumes over a wide range of temporal and spatial scales, as is conceptually visualized in Figure 1. The multiscale nature of deep-sea mining sediment plumes and the importance of understanding and modeling their behavior to determine their potential extent together make for a particularly challenging and complex research topic—one that is greatly informed by existing knowledge but also requires new fundamental understanding and improved modeling capabilities in the field of environmental fluid mechanics.

In addition to the dynamics of sediment plumes, which are the primary focus of this review, fluid mechanics inevitably plays a central role in many other technological, operational, and

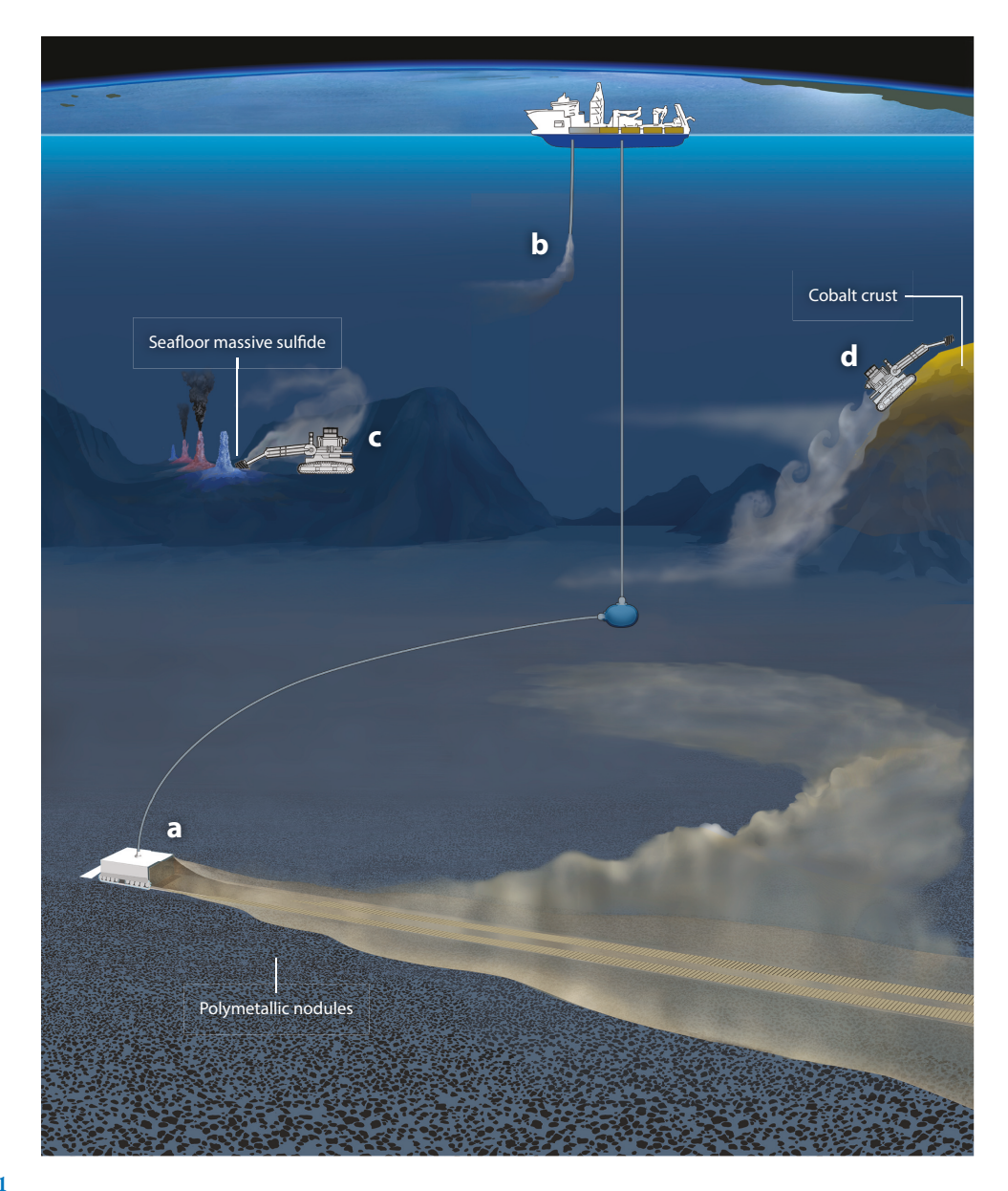


Figure 1

Artist's rendition of three different types of proposed deep-sea mining and associated sediment plumes (note that the plumes and vehicles are not drawn to scale, and mining activities occur in very distant geographic locations). (a) A polymetallic nodule mining operation using a single collector vehicle and (b) possible associated return water discharge. (c) A seafloor massive sulfide mining operation around a hydrothermal vent site. (d) A cobalt crust mining operation on the flank of a seamount.

environmental aspects, given that deep-sea mining operates in the ocean environment. Examples include the design of mining systems, the rheology of sediment-laden flows, the flocculation and settling behavior of sediment, and the vortex-induced vibrations of 4,500-m-long risers. Indeed, the puzzle of why polymetallic nodules lie uncovered on the abyssal plains rather than being buried under meters of sediment (Mewes et al. 2014) may have a simple fluid mechanical explanation.

Discharge phase: the phase in which plume dynamics are dominated by the initial release conditions

Buoyancy-driven phase: the phase in which plume dynamics are driven by a combination of buoyancy forces and interaction with background ocean conditions

Passive-transport
phase: the phase in
which the plume is
passively advected by
background ocean
currents and is
subjected to sediment
settling and
background ocean
turbulence

Collector plume: the plume that forms following the resuspension and discharge of sediment by a nodule collector vehicle

Return plume: the plume that forms following the discharge of sedimentladen water into the water column from a surface operational vessel

Internal wave: a gravity wave that propagates within a

stratified fluid

Polydispersity: the variability in size and shape of individual particles and the flocs of particles that can form due to the action of cohesive forces Altogether, advancing understanding of the fluid mechanics of deep-sea mining will be critical to inform decisions by international governance, contractors, and, more broadly, society in the years to come.

#### 2. SEDIMENT PLUMES

The evolution of sediment plumes associated with deep-sea mining can be broadly divided into three different phases. First is the discharge phase, which is characterized by the dominant effect of inertial and turbulent processes in the immediate vicinity of the mining equipment. Second is the buoyancy-driven phase, in which the negative buoyancy incurred by the suspended sediment and any persistent induced turbulence interact with the surrounding ocean environment. Third, and last, is the passive-transport phase, which is characterized by the passive advection of a dilute plume by background currents, horizontal and vertical diffusion by ambient turbulence, and the settling and deposition of the sediment. While the spatial and temporal scales associated with each of these three phases increase from the discharge to the passive-transport phase, from centimeters and seconds to potentially hundreds of kilometers and years, respectively, the scales at which transitions occur between different phases (and indeed the existence of all three phases) depend heavily on the design and operation of the mining equipment and the encompassing environment parameters. Section 2.1 first introduces the geophysical setting of the sediment plumes. Then, the evolution of benthic collector plumes generated by a nodule mining operation (Figure 1a) is the focus of Section 2.2; potential associated midwater return plumes (Figure 1b) are the focus of Section 2.3. Sediment plumes that are specific to SMS or cobalt crust mining (Figure 1c,d), which are currently less studied, are the focus of Section 2.4.

#### 2.1. Geophysical Setting

The geophysical setting for deep-sea mining sediment plumes differs markedly among nodule mining, SMS mining, and cobalt crust mining. Background currents in the abyssal ocean where nodules are found are generally O(1) cm s<sup>-1</sup>, with a notable tidal component (Aleynik et al. 2017). These currents can be variable in magnitude and direction over a range of space spatiotemporal scales due to a combination of several physical processes, such as remotely generated eddies (Richardson et al. 1993, Aleynik et al. 2017, Purkiani et al. 2020) and internal waves excited either by surface wind forcing (i.e., near inertial waves) (Alford et al. 2016) or by tides interacting with abyssal bathymetry (van Haren 2018). The potential influence of benthic storms, periods of elevated benthic current velocities, in the CCZ serves as a pertinent example of the need for better characterization of the physical oceanography of areas proposed for nodule mining activities (Kontar & Sokov 1994, Aleynik et al. 2017). For regions rich in SMS deposits and cobalt crusts, the associated physical oceanography is dominated by the role of their generally more abrupt and complex bathymetry than is found in abyssal plains, in particular on turbulence production (van Haren 2019). This is explored in more detail in Section 2.4.

For nodule fields, the sediment found in the top layer of the seabed is generally composed of polydisperse clay and silt, with characteristic particle sizes ranging from a few micrometers to a few hundred micrometers, and settling velocities that span several orders of magnitude, typically in the range of O(0.1-10) mm s<sup>-1</sup> (Gillard et al. 2019). The particle size distribution and degree of polydispersity vary geographically, but in general the sediment is conducive to flocculation. A variety of terminology is used to describe the process of individual mineral particles coming into contact and remaining attached. Here, the term flocculation is used to refer to the general process by which particles of clay and silt come into contact and coagulate, with the term coagulation specifically referring to the combined and opposed actions of long-range ionic electrostatic

repulsive forces and short-range London-van der Waals attractive forces that lead to the particles remaining attached (Derjaguin et al. 1987). The term aggregation is understood to encompass processes of aggregate formation other than coagulation (Concha A 2014, Gillard et al. 2019, Zhao et al. 2021). The top layer of seabed sediment, in which the partially or fully buried polymetallic nodules rest, is a highly fluidized mushy layer with volume fractions of sediment of approximately 20-30%. Characterization of sediment properties, and in particular the settling velocities of individual particles and of the porous flocs that they can form, is particularly challenging (Gillard et al. 2019). The shear and turbulence experienced by the suspension depend greatly on the mining and collection mechanisms, which often involve highly turbulent jets for nodule mobilization. The formation or breakage of flocs (Zhao et al. 2021) after resuspension is therefore dependent on the design and is poorly understood and generalizable. There is therefore an urgent need for in situ measurements of sediment properties at various stages of the evolution of sediment plumes. These questions are further explored in Section 3.1. Much less is known about particle properties in SMS and cobalt crust mining scenarios, as the mining technology itself plays a crucial role in setting the nature of the produced fines. By analogy with cutter suction dredging, estimates of the fraction of fines (<63 µm) produced by cobalt crust mining have been used to infer sediment properties (Spearman et al. 2020). This cannot be generalized, however, and technology-specific assessment of particle properties is required for the modeling of SMS and cobalt crust mining sediment plumes.

#### 2.2. Collector Plumes

In this section, the three phases of the evolution of collector plumes and the key associated physics are discussed.

**2.2.1.** Discharge phase. How much sediment is mobilized, and via what physical processes, depends markedly on the design and operation of the nodule collection technology. Often, broad details of proposed technologies are released, sometimes accompanied by unverified claims of minimizing sediment mobilization, when in reality existing knowledge needs to be verified or adapted, or new research is needed. Nonetheless, the designs for proposed nodule collector vehicles under active investigation currently rely on either a hydrodynamic or mechanical pickup mechanism to collect polymetallic nodules that rest on the seabed. In so doing, they disrupt the top layer of the sediment bed, forming a dense, highly turbulent sediment suspension that is carried along with the nodules into the collector. The nodules are then separated from the bulk of the suspension via some internal separation mechanism and transported upward to a surface operational vessel via a vertical transport system, carrying with them a portion of the suspended sediment plus whatever sediment remains stuck to the nodules; the fate of this sediment is discussed in Section 2.3. The majority of the sediment mobilized by the nodule pickup process, however, is discharged in the vicinity of the collector (Figure 2), along with any pumped water that is used to process the nodules through the collector. A smaller but potentially nonnegligible amount of sediment is also expected to be mechanically resuspended by the collector tracks (Muñoz-Royo et al. 2022), further contributing to the sediment plume that forms in the immediate vicinity of the collector wake. In the following discussion, we consider the discharge phase of the sediment plume for the case of a single nodule collector designed to pick up a quantity of nodules on the order of 3 million dry tons per year, a number often cited as being required for the viability of commercial-scale operations (Sharma 2017).

The three competing processes that are primary considerations for influencing the sediment plume in the discharge phase, in the immediate vicinity of a nodule collector, are (a) the turbulent wake produced by the collector itself, which tends to mix the plume upon its discharge; (b) the

#### Mushy layer:

the upper several centimeters of the abyssal seabed, which can be in excess of 70% water (and thus less than 30% sediment) and therefore highly mobile

## Commercial-scale operations:

a commercial nodule mining operation is estimated to require collection of around 3 million dry tons of nodules per year

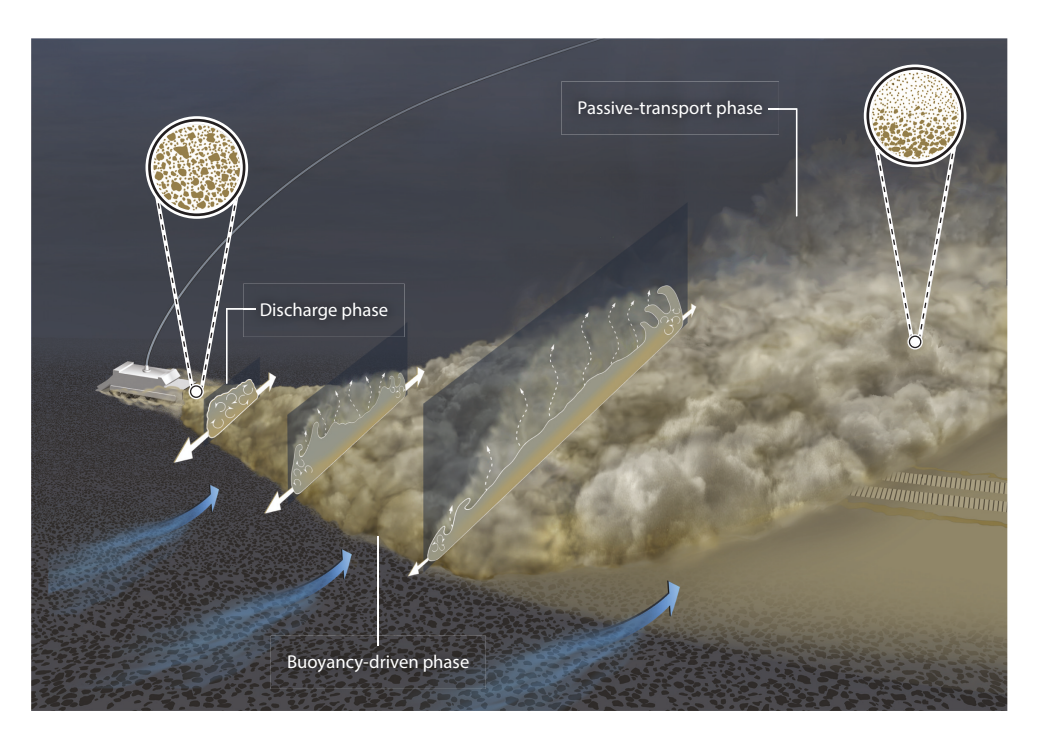


Figure 2

Artist's rendition of the discharge, buoyancy-driven, and passive-transport phases of a nodule collector plume. An initially turbulent wake mixes the collector discharge, which then spreads as a turbidity current to either side of the collector tracks before becoming passively advected by background ocean currents.

Collector Reynolds number (Re<sub>c</sub>): characterizes the strength of inertial forces relative to viscous forces in the collector wake

Outflow Reynolds number (Re<sub>o</sub>): characterizes the strength of inertial forces relative to viscous forces in the outflow iet

Outflow Froude number (Fr<sub>o</sub>): characterizes the ratio of inertial to buoyancy forces in the outflow

turbulent jet produced by the discharge outflow, which tends to advect sediment while entraining ambient fluid; and (c) the negative buoyancy of the discharge, which tends to drive a buoyancy flow toward, and along, the seabed (Jankowski et al. 1994). The relative importance of these three processes can be understood from dimensional analysis arguments, which we base on a simplified model of the collector discharge characterized by six dimensional parameters: the collector velocity  $U_c$ , the outflow velocity  $U_o$ , the reduced gravity of the discharge g', the characteristic height of the collector  $H_c$ , the characteristic diameter of the outflow  $D_o$ , and the kinematic viscosity  $\nu$ . Here, the reduced gravity is defined as  $g'=g\frac{\rho_0-\rho_a}{\rho_a}$ , where g is the gravitational acceleration,  $\rho_0=(1-\frac{c_0}{\rho_p})\rho_a+c_0$  is the discharge mixture density,  $c_0$  is the discharge sediment mass concentration (in units of dry mass per volume),  $\rho_p$  is the particle density, and  $\rho_a$  is the ambient fluid density. These six parameters involve two base units and so can be combined to form four independent, nondimensional numbers. The general level of turbulence produced by the collector wake is characterized by the collector Reynolds number  $Re_c = \frac{U_c H_c}{\nu}$ . Similarly, the outflow Reynolds number  $Re_o = \frac{U_o D_o}{\nu}$  characterizes the level of turbulence of the discharge jet produced. The negative buoyancy imparted to the discharge mixture by the dense sediment competes with inertial forces produced by the collector wake and outflow jet. The relative strength of buoyancy in these two scenarios is characterized by a pair of Froude numbers, which can be defined relative to the outflow velocity,  $Fr_o = \frac{U_o}{\sqrt{g'D_o}}$ , or the collector velocity,  $Fr_c = \frac{U_c}{\sqrt{g'D_o}}$ .

The characteristic velocity of a nodule collector vehicle is O(1) m s<sup>-1</sup>, its characteristic height is O(1-10) m, and therefore Re<sub>c</sub>  $\sim O(10^6-10^7)$ . The discharge flow rate  $Q_o = \frac{\pi}{4}D_0^2 U_o$  (the discharge contains a mixture of suspended sediment and ambient water) is estimated to be

O(1) m<sup>3</sup>s<sup>-1</sup>, while the outflow diameter of a full-scale collector vehicle is O(1) m, such that Re<sub>o</sub> ~  $O(10^6)$ . While these numbers can vary depending on design and operation choices, based on current knowledge it can reasonably be expected that the flow rate of the outflow will not exceed the volume being displaced by the collector itself per unit time, such that  $\frac{Re_o}{Re_c} \lesssim 1$ . The high–Reynolds number flow past the bluff body of the collector produces a highly turbulent recirculation region with a length scale on the order of the vehicle height, followed by a system of trailing vortices leading to a region of progressive decay in the turbulence level (Howell 2011, Derakhshandeh & Alam 2019). Full-scale nodule collectors are expected to remove the top 5-10 cm of the sediment layer, producing sediment discharges on the order of 100 kg s<sup>-1</sup> to accompany the 1 m<sup>3</sup> s<sup>-1</sup> typical volume fluxes of discharge water; the sediment mass concentration of the discharged fluid is therefore expected to be on the order of  $\epsilon_0 \sim 100 \text{ kg m}^{-3}$ . Assuming that the sediment particles have a density of  $\rho_p = 2{,}500 \text{ kg m}^{-3}$ , the resulting particle volume fraction is on the order of 4% and the reduced gravity of the discharge is on the order of 0.5 m s<sup>-2</sup>, so typical values of Fr<sub>c</sub> are expected to be O(1), making it clear that both the wake turbulence and the buoyancy of the particle-laden discharge compete, resulting in complex, nonlinear dynamics of stratified turbulent mixing (Figure 2). Although an unlikely scenario, if there were a collector design in which the outflow velocity far exceeded the collector velocity (i.e.,  $\frac{Re_o}{Re_c} \gg 1$ ), the discharge would be characterized by a strong negatively buoyant jet from a moving source, which entrains ambient fluid and loses momentum until the plume transitions to either a buoyancy-dominated flow or a passively advected flow. A 2D study along these lines was performed by Elerian et al. (2021), but the role of motion of the collector and 3D spreading on the resulting discharge was not considered.

A potentially meaningful contribution to the resuspended sediment budget comes in the form of direct resuspension by the collector tracks even in the absence of a discharge. Muñoz-Royo et al. (2022) inferred, from direct observations of the plume produced by a preprototype collector with all collection heads inactive, that resuspension by the collector tracks was less than, yet of the same order of magnitude as, the discharge mass flux with all collector heads active. This indicates that all collector activities on the seabed should be considered as potentially contributing to the release of plumes, and further design-specific experiments need to be carried out to determine the resuspended sediment budget, from both the collector discharge and the collector tracks. The resuspension mechanism and history of the sediment released in the discharge differ markedly from that of the sediment kicked up by driving of the collector alone, which likely affects flocculation, disaggregation, and floc size in the suspension; special attention must therefore be given to in situ characterization of sediment properties in both types of discharges.

**2.2.2.** Buoyancy-driven phase. Following the initial discharge into its turbulent wake, at some distance behind the collector the discharge momentum in the direction of release decreases significantly, and the sediment mass concentration scales as  $\frac{\dot{m}}{U_c A}$ , where A is the vertical cross-sectional area of the plume that is anticipated to scale as  $H_c^2$  in the collector wake, and  $\dot{m}$  is the mass flux of resuspended sediment, which should include both the discharged sediment and the sediment disturbed by driving of the collector. The magnitude of the concentration can be reasonably estimated to be O(1-10) kg m<sup>-3</sup>, which is a disturbance of 0.1% to 1% from the ambient water density (Lavelle et al. 1981). Sediment mass concentrations O(1) kg m<sup>-3</sup>, and even as low as 0.07 kg m<sup>-3</sup>, have been shown to trigger turbidity currents (Hage et al. 2019), which suggests that following the discharge phase, the plume dynamics are buoyancy driven. This is consistent with in situ observations from early mining trials that reported heavy resedimentation 100 m on either side of the collector tracks (Burns 1980), suggesting that a relatively high-concentration, low-lying plume spread laterally away from the tracks as a consequence of density flow (Lavelle et al. 1981; Jankowski et al. 1994, 1996).

#### Collector Froude number (Fr<sub>c</sub>): characterizes the ratio of inertial to buoyancy forces in the collector

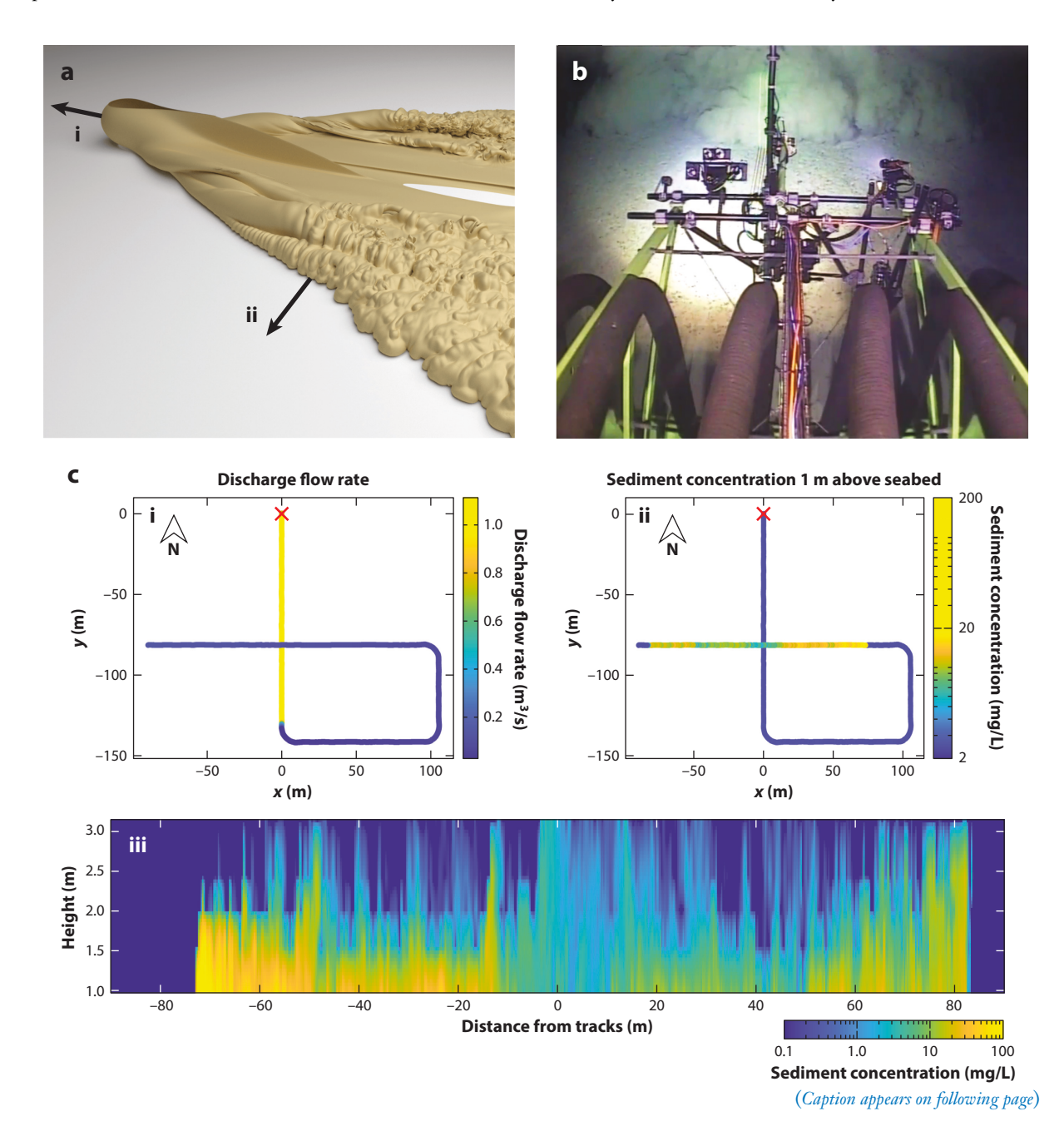
# Turbidity current: a gravity current caused by increased density due to the presence of suspended sediment

The propagation of turbidity currents, the turbulent mixing they generate, and their deposition pattern remain active topics of research (Wells & Dorrell 2021). Turbidity currents are generally characterized by the presence of a high-concentration head followed by a thinner body (Meiburg & Kneller 2010). Shear-induced instabilities at the head generate entrainment of ambient fluid and dilution of the head, which is replenished in particles from the body. As the current dissipates turbulent kinetic energy and the sediment progressively settles, the negative buoyancy of the current is reduced, further favoring the relaminarization of the flow and deposition. Once the current has lost most of its momentum, interstitial fluid can detrain from the current and mix with ambient fluid (Necker et al. 2005; Dorrell et al. 2011, 2013).

A key consideration that is specific to deep-sea mining is that the source of the turbidity current is moving. To gain insight into this, Ouillon et al. (2021) conducted the first investigation of a gravity current continuously released from a moving source using a combination of high-resolution direct numerical simulations, proof-of-concept laboratory experiments, and scaling analysis to rationalize the results. The idealized numerical model did not resolve individual particles and their interactions, settling, or propensity to flocculate but instead used an equilibrium-Eulerian description of a buoyancy scalar to represent the sediment mass concentration. The study considered a spherical source of a density-contributing scalar of diameter D moving close to the bottom boundary at a velocity  $U_c$ . The density excess produced by the source scales as  $\Delta \rho \sim \frac{\dot{m}}{D^3} \tau$ , where  $\tau$  is the characteristic time over which the density-contributing scalar can be accumulated, and the buoyancy velocity is accordingly defined as  $U_b = \sqrt{g \frac{\Delta \rho}{\rho_a} D}$ , where  $\rho_a$  is the ambient fluid density. It was shown that for values of  $\frac{U_c}{U_b}$  < 0.63, the gravity current produced by the moving source propagates more rapidly than the source itself, resulting in the gravity current front overtaking the source in its direction of motion. When  $\frac{U_c}{U_L} > 0.63$ , however, the source always moves more rapidly than the current, and the dense scalar forms a wedge-shaped front behind the source (see **Figure 3***a*); when  $\frac{U_c}{U_b} > 1$ , the dense fluid that forms the head of the gravity current propagates predominantly in the direction normal to that of the moving source. Moreover, the evolution is similar to that of a short-release gravity current and can be reasonably approximated by a simple box model in a vertical plane normal to the direction of motion of the source (see, for instance, Harris et al. 2002). A 10-m-wide, large-scale nodule collector moving at 0.5 m s<sup>-1</sup> can be expected to discharge on the order of 60–300 kg s<sup>-1</sup> of sediment in its wake, resulting in a  $\frac{U_c}{U_h}$  ratio of 0.6–1. The regime transition of the moving source turbidity current is therefore likely to be relevant to deep-sea mining nodule collectors, and design and operational choices can markedly influence the dynamics of the plume in the buoyancy-driven phase.

Muñoz-Royo et al. (2022) conducted the first field experiments to directly measure the turbidity current produced by the discharge of a moving collector vehicle. The experiments, which were performed at a depth of 4,500 m in the CCZ region of the Pacific Ocean, were consistent with predictions of the idealized model of Ouillon et al. (2021). A realistic disturbance was generated by a preprototype mining vehicle, and the resulting turbidity current was measured by driving the specially instrumented collector in a selfie maneuver, concluding with the vehicle traveling in a direction orthogonal to the mining tracks, through the plume it had recently created (Muñoz-Royo et al. 2022). Selfie maneuvers consist of the nodule collector driving in a straight line while actively mining, then turning off its collection system, operating three successive 90° turns, and proceeding to intersect its own plume to measure its properties. The in situ observations of the turbidity current (see **Figure 3***b,c*) demonstrated that the disturbance traveled for more than 100 m on either side of the track, in line with the observations of resedimentation by Lavelle et al. (1981). The turbidity current head was found to reach heights of approximately 3 m above the seabed, with the front of the current reaching velocities of tens of centimeters per second soon after release. As anticipated (Jankowski et al. 1994), the turbidity current was initially able to travel against

cross-flow components of the background current, on the order of 5 cm s<sup>-1</sup>. It was also found that the cross-flow component interacted nonlinearly with the against- and along-current turbidity current fronts; the turbidity current propagating with the cross-flow component tended to have a taller, more sharply defined head, while the turbidity current propagating against the cross-flow tended to have a thinner, less sharply defined head. In reasonable agreement with laboratory experiments (Hallworth et al. 1998), the center of mass of the turbidity current was translated by



(a) A 3D rendering of the wedge-shaped gravity current released from (i) a moving source, showing (ii) the lateral propagation of a highly turbulent gravity current front (Ouillon et al. 2021). (b) Image from a forward-facing camera mounted on a preprototype nodule collector showing the head of the approaching turbidity current generated by the sediment discharge during a selfie experiment (Muñoz-Royo et al. 2022); the experiments were conducted in situ at a depth of 4,500 m in the Clarion-Clipperton Zone. (c) A selfie experiment in which the preprototype nodule mining collector intersected its own plume soon after discharge; the collector drove the loop pattern starting from the red cross. The collector track pattern is illustrated for a selfie colored by the (i) discharge mass flow rate and (ii) measured sediment mass concentration 1 m above the seabed ahead of the vehicle, showing when and where the plume was produced and observed, respectively. (iii) Time series of the vertical profile of the sediment mass concentration measured over the final leg of the selfie track, showing the turbidity current formed by the plume on either side of the collector tracks (note that this is not a snapshot but reveals spatiotemporal evolution). Panel c adapted from Muñoz-Royo et al. (2022).

approximately 60% of the cross-flow component of the background current, reflecting the highly nontrivial interaction of the background current with the dense flow.

The sediment budget, i.e., the mass of sediment that remains in suspension relative to the initial discharge, is governed in the buoyancy-driven phase by depositional processes within the turbidity current. Burns (1980) reported heavy redeposition up to 100 m away from the tracks following mining trials, suggesting that a significant fraction of the sediment discharged by the collector deposited locally from the low-lying density flow. During the large-scale field experiments of Muñoz-Royo et al. (2022), from 2% to 8% of the sediment mass discharged was detected 2 m or higher above the seabed and was not observed to settle over several hours, while the remaining 92–98% of the sediment mass was below 2 m, with some fraction of that being deposited locally, causing the blanketing of nodules on the seabed. However, there is no guarantee that the sediment still in suspension below 2 m settled further, owing to vertical transport by ambient turbulence, and the actual suspended and deposited mass budget of sediment following the turbidity current phase remains unquantified.

There is currently no predictive model for the sediment budget. Turbulent mixing in the canonical problem of a lock-release turbidity current is an active research area (Wells & Dorrell 2021), and the deposition and detrainment processes in the framework of deep-sea mining depend nontrivially on the characteristics of the discharge, sediment properties, topography, background currents, and background turbulence. While Ouillon et al. (2021) do not address the question of the spatial distribution of sediment that results from the turbidity current, their research opens a promising avenue for systematically characterizing the fraction of sediment that, through a combination of shear-driven mixing, differential settling, and interaction with background currents and turbulence, is unable to deposit locally in the near-bottom plume and becomes passively advected by background currents, a process we refer to as detrainment. Indeed, the findings of Ouillon et al. (2021) suggest that the lock-release or dam-break laboratory and numerical experiment, which has been extensively used to investigate rectilinear gravity and particle-driven currents (e.g., Hallworth et al. 1993, 1996; Gladstone et al. 1998; Maxworthy et al. 2002; Necker et al. 2005), is suitable for the investigation of detrainment from the moving collector turbidity current. Ultimately, however, direct in situ monitoring of the buoyancy-driven phase of collector plumes remains a necessity, and such monitoring must account for the intrinsically transient and spatially heterogeneous nature of such flows, which further complicates the assessment of the initial conditions of the passive-transport phase.

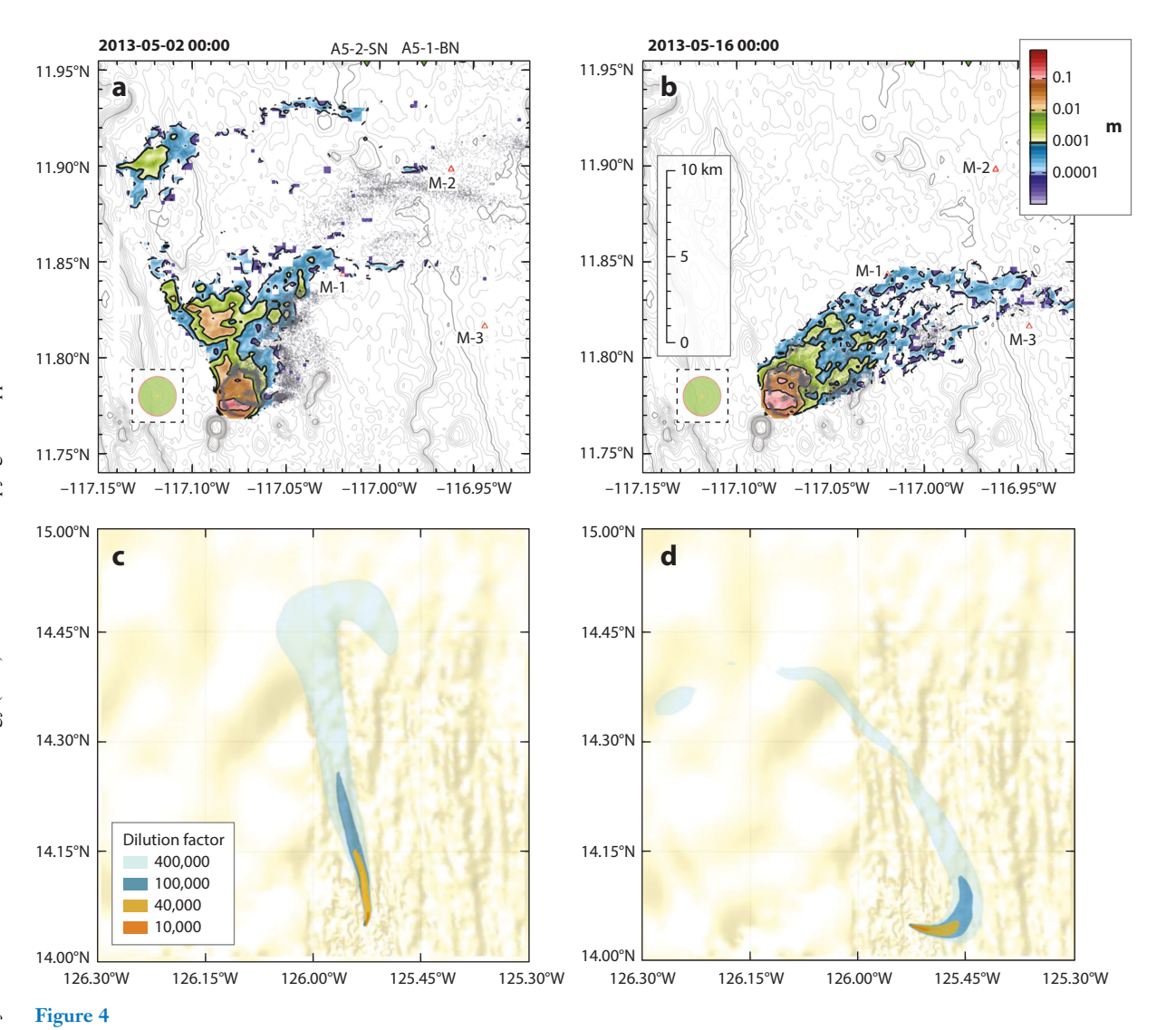
Finally, turbidity currents in geophysical settings can sometimes travel long distances in regions of weak downward slope, the mechanisms of which remain a vigorously debated topic that is pertinent to investigations of the buoyancy-driven phase of nodule collector plumes (Blanchette et al. 2005, Kneller et al. 2016, Luchi et al. 2018, Dorrell et al. 2019, Wells & Dorrell 2021). While the sediment discharges of a full-scale deep-sea mining operation are small compared to large

turbidity events generated by storms or earthquakes, which can lead to the resuspension of several cubic kilometers of sediment (Meiburg & Kneller 2010), the potential for autosuspension and self-acceleration mechanisms to affect collector sediment plumes is an important open question, as it could add substantially to the overall budget of suspended sediment.

**2.2.3.** Passive-transport phase. The discharge phase and buoyancy-driven phase set the initial conditions for the passive-transport phase of the collector plume. This phase of transport (Figure 2) is characterized by the dominant role of the ocean currents in advecting the sediment. By definition, this phase is concerned with sufficiently low sediment mass concentrations such that buoyancy no longer plays a dominant role in transporting the sediment. A slowly varying background benthic current primarily serves to create a meandering path of particles, transporting them away from their position at the end of the buoyancy-driven phase. Turbulent diffusion then progressively dilutes the sediment plume as it is advected, resulting in an increasingly wide and tall plume of generally decreasing concentration. Furthermore, as a result of spatial variations in the fluid velocity, advection further induces dispersion, stretching the plume and augmenting the effect of turbulent diffusion in diluting the plume. Finally, given that the particles that make up the plume are denser than the ambient fluid, the sediment settles, with sediment particles and flocs of different sizes and porosities settling at different rates; this process is in competition with background vertical turbulent diffusion that acts to maintain sediment in suspension. Predicting the ultimate fate of a sediment plume in the passive-transport phase demands that all these processes be accurately accounted for over long periods of time and large spatial distances. Other processes, such as sediment flocculation (Gillard et al. 2019) and biogenic scavenging of sediment, could be considered (Rolinski et al. 2001), but given the highly dilute nature of the plume that is expected to result from the buoyancy-driven phase and the challenging conditions of the abyssal ocean, such processes seem likely to be insignificant in the passive-transport phase.

To date, the passive-transport phase of a collector plume has been the subject of most of the attention for deep-sea mining sediment plumes. Historical efforts have often relied on large-scale numerical models that make necessary, but unfounded, assumptions about the initial form of the plume coming from the vicinity of the collector (i.e., the discharge and buoyancy-driven phases) and partially resolve the physics of both the fluid motion, solving some form of the continuity and momentum equations, and the physics of the plume, via Eulerian or Lagrangian transport models. A hydrostatic model was used to resolve the velocity field and transport of a collector plume over 1 week (Jankowski et al. 1996), and subsequently a nonhydrostatic version of the model was used in a smaller but higher-resolution domain (Jankowski & Zielke 2001). The latter study compared sedimentation rates with field data, with poor agreement, stressing the need for a better characterization of the benthic boundary layer to inform the model. A nonhydrostatic simulation of plume dispersion over a 5-week period in the Eastern German area of the CCZ showed that oscillations induced by wind and geostrophic shear, tidal forcing, and the passage of mesoscale ocean eddies can all comparably contribute to the current and turbulent mixing variability in the abyssal ocean (Aleynik et al. 2017). Turbulence levels in particular were seen to be markedly affected by the passage of remotely generated eddies and by topographically induced internal wave breaking even in thick bottom boundary layers, an observation consistent with in situ turbulence measurements (van Haren 2018). Furthermore, changes in background ocean currents induced by externally generated eddies were shown to have a marked effect on the trajectory of a collector plume and the resulting deposition pattern, as exemplified in Figure 4a,b. Several other such simulations have been performed by Gillard et al. (2019), Spearman et al. (2020), and Purkiani et al. (2021), the former accounting for potential flocculation effects.

#### Turbulent diffusion: the effective diffusion of the sediment mass concentration caused by small-scale fluid dynamical processes in



(a,b) Map of deposited (colored areas) and suspended (black dots) particles from a collector plume transport simulation using a Lagrangian particle transport model. The presence (a) and absence (b) of a mesoscale eddy during the period of simulation show how important advection by background currents is in determining the deposition map. Panels a and b adapted from figure 5 of Aleynik et al. (2017). (c,d) A 3D numerical simulation of a continuous commercial-scale midwater return plume over 90 days: top view of the dilution factor contours of the plume for a prevalent current (day 36 of the simulation) (c) and a current transition (day 88 of the simulation) (d). These contours show the maximum horizontal extent of each 3D contour level and are not a cross section at a specific depth. Panels c and d adapted from Muñoz-Royo et al. (2021); data generated by International Marine and Dredging Consultants.

While the aforementioned numerical models of transport can provide valuable information about plume evolution over specific time periods and for specific operational and physical oceanography conditions, several key issues, some physical and some numerical, need to be addressed for such models to reliably handle the deep-sea mining problem. To date, models have not based their initial conditions on information from the discharge and buoyancy-driven phases, nor could they directly capture the physics of these regimes (e.g., turbidity currents). And yet

their ability to reasonably model the extent of a collector plume is profoundly influenced by these choices. For example, observations have suggested that O(90%) of disturbed sediment may return to the seabed locally (Lavelle et al. 1981), as opposed to assumptions that all picked-up sediment goes into suspension in the bottom few meters of the ocean above the seabed (Aleynik et al. 2017), which could lead to an order of magnitude error in the ultimate extent of the plume. Another issue for numerical approaches is that the sediment mass concentrations that can potentially impact the local ecosystem remain poorly quantified, such that until impact thresholds are clearly identified, sediment plumes need to be tracked down to very low concentrations, close to background levels on the order of 10 µg L<sup>-1</sup> (Gardner et al. 2018). As a result, the evolution of the plume needs to be modeled over potentially long durations, during which the sediment may be advected over distances of tens to hundreds of kilometers. In such cases, numerical models based on an Eulerian description of the concentration field often face the challenge of either underresolving the sharp vertical gradients over distances O(1-10) m that arise from the initially low-lying plume at the end of the buoyancy-driven phase or suffering from excessively long computational times. Underresolving the vertical gradients of concentration leads to numerical diffusion that far exceeds the vertical turbulent diffusion of the benthic boundary layer, which plays a crucial role in interacting with sediment settling and in setting the vertical extent of the plume (Ouillon et al. 2022b). Aside from the challenges of plume transport modeling, accurately predicting mesocale and submesoscale features in regional models remains highly nontrivial, and models are still being actively developed (Lermusiaux et al. 2013).

The role of polydispersity is also a critical consideration, as it has been shown to be one of the most important factors in determining the extent of sediment plumes in the passive-transport phase (Ouillon et al. 2022b). In an Eulerian description of sediment mass concentration, polydispersity is accounted for by dividing the concentration field into N scalar quantities, each associated with a given settling velocity. As a result, models that take such approaches are typically limited to a small number of settling velocities to limit the increase in computational cost associated with solving the transport equation for many scalar quantities. Alternatively, as in the work of Spearman et al. (2020), Lagrangian and hybrid Eulerian-Lagrangian approaches (Yeh 1990, Devkota & Imberger 2009) can be used that consider the discrete release of a large number of individual particles that are advected by the flow-field solution and that account for turbulent diffusion through some diffusion model, typically a random walk. This has the clear advantage that each released particle, which can represent a certain mass of sediment (see, e.g., Aleynik et al. 2017), can admit a different settling velocity without a significant increase in computational cost. The downside is that a large number of particles needs to be used for every different settling velocity so that diffusion processes can be reasonably approximated by random-walk models. Given that this approach requires particles to be continuously released from the mining area, the total number of particles that need to be tracked with such approaches can rapidly become significant, requiring well-optimized transport models.

Through a combination of accurate modeling of physical oceanography, which accounts for the many physical processes that affect background currents and turbulence in the deep ocean, and modeling of plume transport, which accounts for the challenges of resolving the sharp gradients of the sediment mass concentration over long periods of time, numerical models can look to capture the far-field evolution of deep-sea mining plumes with some accuracy, provided that they are parameterized with, and validated against, in situ data. An overarching challenge, however, is that the panoply of abyssal oceanographic conditions encountered produces transport processes that are highly complex and variable in nature. This profoundly influences the spatial and temporal evolution of sediment plumes, making general statements about plume extent from

Numerical diffusion: artificial diffusion induced by discretization in a numerical model; for simulations of deep-sea mining sediment plumes, numerical diffusion can initially exceed true physical diffusion, rendering predictions inaccurate Settling Péclet number: the ratio of the rate of advective transport by settling to diffusive transport such models challenging, and so such models remain ill-equipped to answer broader questions of plume extent at the scale of many operations.

An alternative approach that builds on the pioneering work of Lavelle et al. (1981), which relies on fundamental principles of transport phenomena, was considered by Ouillon et al. (2022a,b) for the passive-transport phase of both midwater return plumes and collector plumes. They developed a fundamental model that considers the advection, diffusion, and settling of polydisperse plumes in a system that is dominated by advection in the direction of the background currents, turbulent diffusion in the horizontal direction normal to the currents, and a combination of differential settling and turbulent diffusion in the vertical direction. By design, and in contrast to a complex numerical simulation, the model allows the relatively straightforward calculation of impact metrics based on a concentration threshold that characterizes the extent of plumes over very long timescales. A key distinction is made between more traditional Eulerian extent metrics, such as the instantaneous volume of fluid that exceeds a certain concentration threshold, and so-called Lagrangian metrics, such as the volume of fluid that ever exceeds a threshold produced per unit time. Such disambiguation is critical, as the former can reach a quasi-steady state under slowly varying oceanic and operational conditions and therefore does not increase indefinitely, while the latter linearly accumulates with time. A key finding is that the competition between settling and vertical turbulent diffusion plays a central role in setting the extent of a collector plume for a given concentration threshold, and that this competition, characterized by the vertical settling Péclet number, affects the impact metrics in a highly nonlinear fashion. Furthermore, the findings of Ouillon et al. (2022b) reinforce the need for accurate in situ technology and operation-specific measurements of the particle size and particle velocity distributions of the sediment at different phases of plume evolution.

#### 2.3. Return Plumes

A fraction of the sediment picked up by a nodule collector vehicle is expected to be carried with the nodules by a vertical transport system, either in suspension or stuck to the nodules, up to the surface operation vessel (Figure 1). On the surface vessel, the nodules are cleaned in preparation for shipping to land-based processing facilities, and several strategies are considered for dealing with the resulting sediment-laden water. Due to the quantities of sediment involved, some deem it impractical to store this water on the surface vessel to be taken ashore for handling. Furthermore, a surface discharge of the water is widely considered to be too environmentally challenging to be viable. As such, there are three discharge strategies under consideration. One strategy is to release the unwanted sediment-laden water as a return plume in the midwater column, typically well below the ocean's surface mixed layer yet far above the seabed, the aim being to achieve significant dilution on acceptable length, time, and volume scales (Figures 1b and 5). Another option is a near-bottom release, with the aim of depositing the sediment somewhat locally on the seabed in a region that has already been impacted by the collector operations. Finally, there is the possibility of sending this sediment-laden water back through the collector vehicle to become part of the collector plume. Currently, there is no consensus as to which return strategy would produce a plume with the least environmental impact. If the return water was directed back through the collector vehicle, becoming part of the benthic collector plume, the scenario is as discussed in Section 2.2; the return water would likely have a significant impact on the properties of the discharge from the collector, in turn influencing the extent of the subsequent collector plume development. In the following, the fluid dynamics of a midwater return plume are discussed, with the less studied case of a near-bottom return plume being briefly addressed as a scenario in Section 2.3.2. As with the benthic collector plumes, three phases of evolution are considered: the discharge phase, the buoyancy-driven phase, and the passive-transport phase.

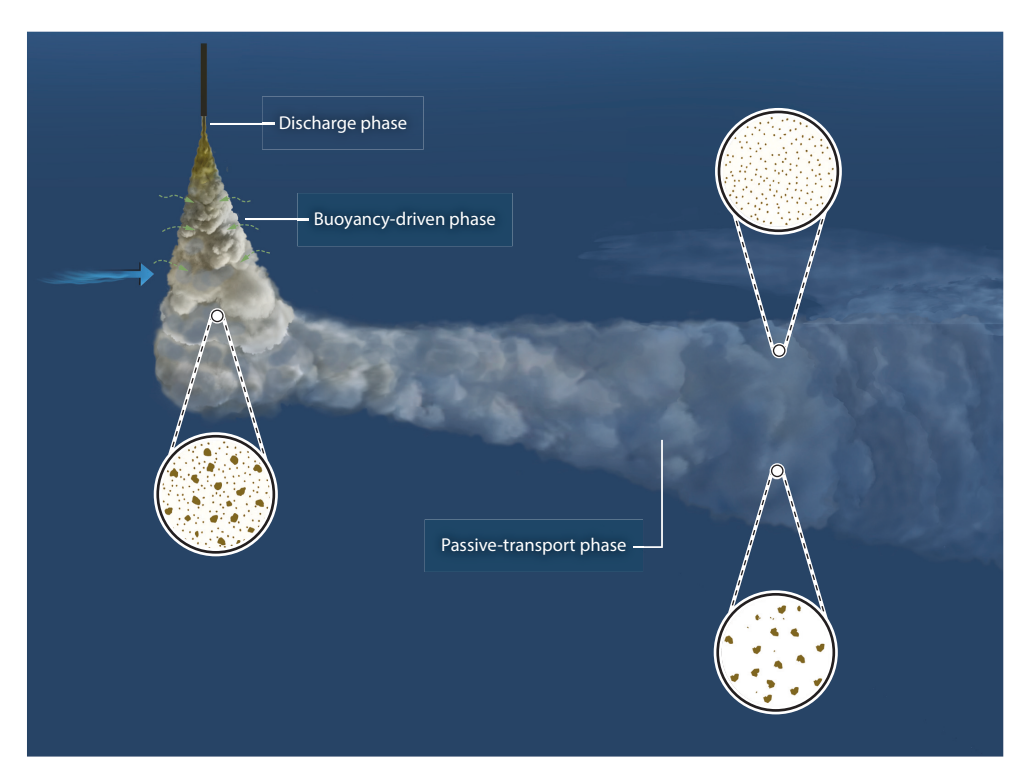


Figure 5

Artist's rendition of the discharge, buoyancy-driven, and passive-transport phases of a midwater return plume. There is substantial turbulent entrainment into the initially negatively buoyant plume, which descends to a level of neutral buoyancy before becoming passively advected by background ocean currents and undergoing differential settling.

In contrast to collector plumes, buoyant turbulent jets and plumes in stratified environments are ubiquitous in geophysical fluid dynamics and as such have been extensively studied (Morton et al. 1956, List 1982), with the role of sedimentation in particle-laden plumes having been further investigated in the context of volcanic ash clouds and hydrothermal vents (Sparks 1986, Ernst et al. 1996; reviewed in Woods 2010). The evolution of a midwater return plume immediately after discharge from a pipe and in the following buoyancy-driven phase is therefore well-described by existing jet and buoyant plume models (Morton et al. 1956), which have been advanced for application by accounting for factors such as sedimentation or the presence of a background cross-flow (Ernst et al. 1996, Lee & Chu 2003, Devenish et al. 2010). While such models adequately capture the discharge and buoyancy-driven phases of midwater return plumes, which set the initial condition for the more challenging passive-transport phase, the key physics and scaling of the former are presented in the following.

**2.3.1. Discharge phase.** The canonical configuration for the discharge of a midwater return plume is that of a downward-facing pipe (**Figure 5**). Based on the expected operational parameters for a midwater discharge (Oebius et al. 2001), the characteristic discharge velocity of a midwater return plume is  $U \sim O(1)$  m s<sup>-1</sup>, the pipe radius is  $r \sim O(10^{-1})$  m, and the sediment volume fraction is  $\varphi \sim O(10^{-2})$ , the latter establishing that the kinematic viscosity remains  $v \sim O(10^{-6})$  m<sup>2</sup> s<sup>-1</sup>. It follows that the Reynolds number of the discharge Re =  $\frac{Ur}{v}$  is  $O(10^5)$ , and the emerging, fully developed, turbulent flow initially can be idealized as a top hat profile that evolves over a

Dilution factor: the degree to which the initial discharge of sediment-laden water is diluted by entrainment during the buoyancy-driven phase distance of approximately 10 radii into a self-similar profile throughout the so-called zone of flow establishment (ZFE) (Ernst et al. 1996, Lee & Chu 2003). After the ZFE, the subsequent evolution of the plume depends on the local Froude number,  $Fr = \frac{w}{\sqrt{g'b'}}$ , where w is the centerline velocity, g' is the reduced gravity, and b is the plume radius (Morton et al. 1956, Ernst et al. 1996, Lee & Chu 2003). Any flow produced by a continuous source of buoyancy is expected to behave like a buoyancy-driven plume at large enough distances, even if it starts out as a momentum-driven jet (Lee & Chu 2003). The distance of a jet-to-plume transition is governed by the momentum length scale  $l_s = M_0^{3/4}/B_0^{1/2}$ , where  $M_0$  is the initial momentum flux and  $B_0$  is the initial buoyancy flux; for distances less than  $l_s$ , the system behaves as a jet, and for distances greater than  $l_s$ , it behaves as a plume. Since  $l_s \sim O(1)$  m for the deep-sea mining scenario, a midwater return plume will be almost immediately dominated by buoyancy following release (**Figure 5**).

**2.3.2. Buoyancy-driven phase.** After a short jet-like phase, the midwater return plume enters a predominantly buoyancy-driven phase. The presence of a background stratification continually reduces the buoyancy flux of the plume and thus can play a central role in setting its vertical extent, as characterized by the buoyancy number  $\Delta = \frac{N^2 w^2}{g^2}$ , where N is the characteristic background buoyancy frequency (Lee & Chu 2003). The buoyancy flux decreases to zero at a height of neutral buoyancy, but due to inertia the plume will overshoot this level, forming a dome that then rebounds up to form a lateral intrusion (**Figure 5**). The vertical extent of the plume scales as  $z_e \sim 4B_0^{1/4}N^{-3/4}$ , the dilution factor scales as  $S \sim Q_0^{-1}B_0^{3/4}N^{-5/4}$ , and the thickness of the intrusion at the horizontal spreading depth scales as  $b_e \sim 1.7B_0^{1/4}N^{-3/4}$ , being around 40% of the vertical extent of the plume (Lee & Chu 2003). Given typical values for an ocean plume release, it is found that  $z_e \sim 10^2$  m and  $S \sim 10^{-3}$  (initial dilution by a factor of 1,000), with the resulting lateral intrusion being several tens of meters thick. The scaling analysis of the buoyancy-driven phase thus reveals that by the time the midwater return plume intrudes at the point of neutral buoyancy, it will have experienced significant dilution.

The role played by settling of the dense suspended sediment in the buoyancy-driven phase can be neglected if the sediment settling velocity  $v_s$  is very small compared to the advection velocity scale of the plume, i.e.,  $v_s \ll U \sim (B_0 N)^{1/4}$  (Mingotti & Woods 2020); typically  $v_s \sim$  $O(10^{-4}-10^{-3}) \text{ m s}^{-1}$  and  $U \sim O(10^{-1}) \text{ m s}^{-1}$ , and so this is readily satisfied. James et al. (2022) considered whether the neutrally buoyant sediment-laden water intruding laterally from the base of the discharge plume may further undergo a separation process in which the sediment settles out from the interstitial water, which subsequently rises. Since the thickness of the intrusion is expected to be O(10) m, sediment settling speeds will be  $O(10^{-3})$  m s<sup>-1</sup> or less, and the volume fraction of particles is  $O(10^{-5})$ , this process is not expected to be significant in the presence of other background ocean processes. Contrary to the extensively studied case of positively buoyant particle-laden plumes such as volcanic ash clouds and hydrothermal vents (Woods 2010), the negative buoyancy of midwater return plumes is imparted by the suspended sediment itself, not temperature or salinity differences. Any difference in the temperature or salinity of the discharged plume with the ambient fluid would be small and would become negligible following the rapid dilution of the plume in the buoyancy-driven phase. Recent field and laboratory experiments (Muñoz-Royo et al. 2021, Wang & Adams 2021) confirmed the dynamic behavior of a midwater return plume consistent with the aforementioned plume modeling, verifying that sediment acts as a passive tracer and that settling effects on the dynamics of the plume and intrusion are negligible (see Figure 6a-c). Another key difference with positively buoyant particle-laden plumes is that the mechanism of reentrainment of particles that had settled out of the plume does not apply to midwater return plumes, given that particles settle in the direction of the buoyancy force. Finally, an application of the models was performed by Rzeznik et al. (2019) to investigate the role of

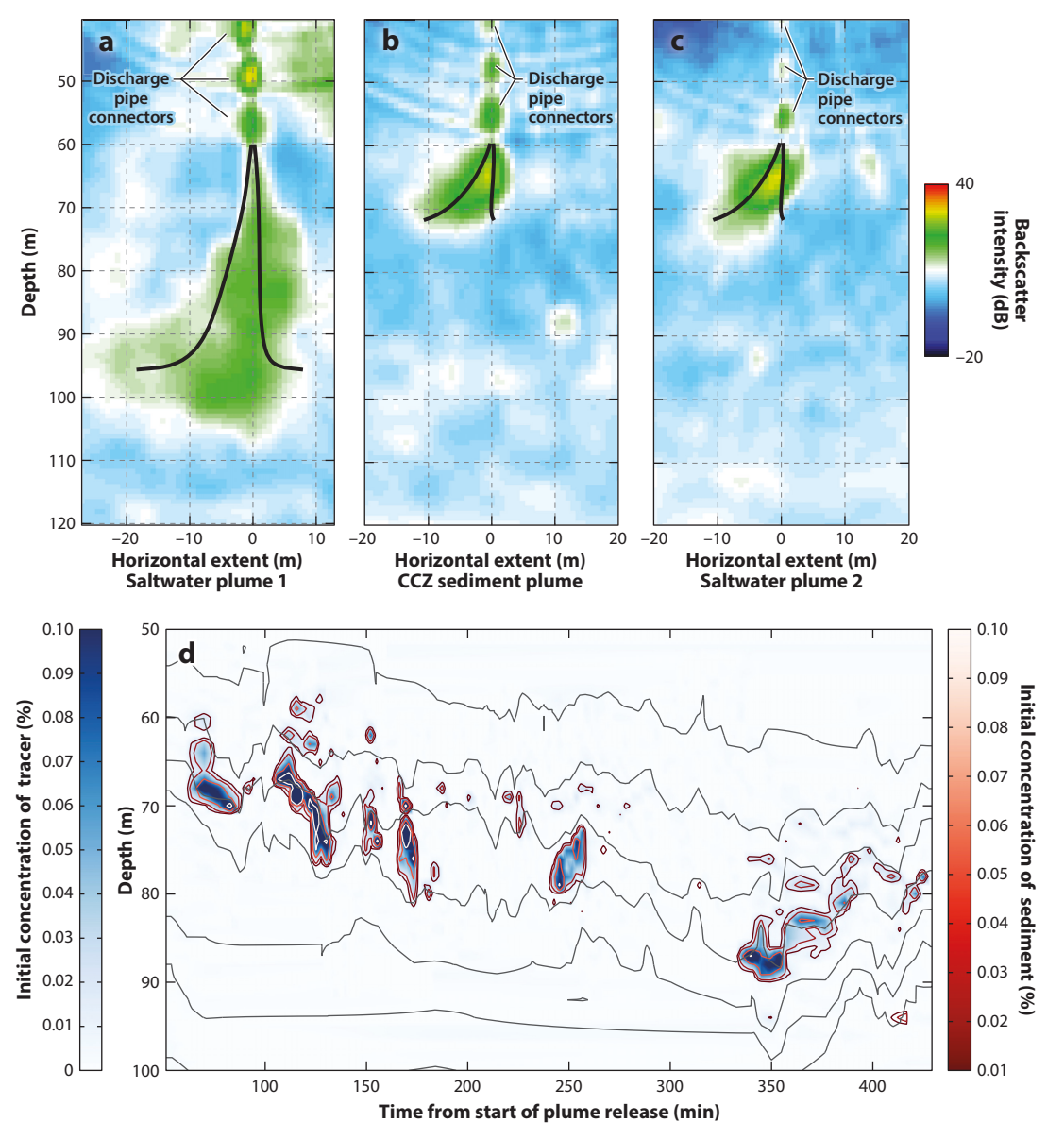


Figure 6

(a-c) Acoustic backscatter intensity images of two saltwater return plumes and one Clarion-Clipperton Zone (CCZ) sediment return plume from the PLUMEX experiments. The superimposed black lines are predictions from the discharge plume model. (d) Tow-yo observations of the CCZ sediment ambient plume, showing time series of the tracer concentration as a percentage of the initial discharge concentration for the CCZ sediment (red isocontours) and dye tracer (blue colored areas) during the passive-transport phase of a PLUMEX Experiment. Black lines are isopycnals. Figure adapted from Muñoz-Royo et al. (2021).

compressibility, which was determined to be negligible for the upper ocean but pertinent for a deep-sea release.

An alternative to a midwater discharge is a near-bottom discharge. Depending on the height of the discharge above the seabed, it may act as an impinging buoyant plume on the seabed, a problem investigated fundamentally by Chowdhury & Testik (2015). The resulting flow initially behaves like an axisymmetric, momentum-driven wall jet before transitioning into an axisymmetric turbidity current, subject to the influence of other environmental factors such as background current and topographic slope. Therefore, the fate of the return plume in the case of the nearbottom discharge is likely tied to the detrainment properties of the resulting turbidity current. It additionally remains unknown whether the plume's impingement on the seabed would resuspend sediment via shear in the top layer of the seabed, thereby increasing the sediment budget of the return plume. For reasons such as these, it is unclear whether a near-bottom release would result in more or less environmental impact than a midwater release, in particular considering that the midwater column and the benthic environment respond differently to perturbations (van der Grient & Drazen 2021).

**2.3.3.** Passive-transport phase. Emerging at a level of neutral buoyancy from the buoyancy-driven phase, the evolution of the passive midwater sediment plume is primarily controlled by advection from background currents, turbulent diffusion, and settling (Ouillon et al. 2022a) (**Figure 5**). The evolution is phenomenologically similar to that of benthic collector plumes, with the exception that deposition on the seabed is a much more distant and distributed scenario. In the absence of other processes, for a given particle-settling velocity  $v_s$ , the characteristic deposition time is  $H/v_s$ , where H is the height above the seabed where the plume reaches neutral buoyancy after the buoyancy-driven phase. For  $H \sim O(10^3)$  m, particles settling at 1 mm s<sup>-1</sup> would take  $\sim$ 11 days to reach the seabed, while particles settling at 0.1 mm s<sup>-1</sup> would take on the order of 4 months to do so. Given that the advection distance of background ocean currents is typically several kilometers per day, it is evident that over the timescales of deposition the plume will be transported large distances and further will experience significant dispersion and dilution en route. This stands in contrast with deposition from collector plumes, which starts to take place in the immediate vicinity of the mining area.

Very limited data exist for the far-field transport of midwater sediment plumes, with most such plume studies being related to natural releases from hydrothermal vents (Baker & Massoth 1986, Nojiri et al. 1989, Resing et al. 2015). Muñoz-Royo et al. (2021) monitored the early stage of the passive-transport phase of a midwater return plume (Figure 6d), finding that the highly diluted, disaggregated sediment remained consistent with a dye tracer over a 6-h observation window, indicating very low settling velocities (<0.05 mm s<sup>-1</sup>); as expected, the passive-transport plume was subject to other background processes such as heaving of the isopycnals and further dilution by background turbulent mixing. The models of Segschneider & Sündermann (1998) and Rolinski et al. (2001) considered a return plume scenario but were very coarsely resolved. A higher-resolution model (Muñoz-Royo et al. 2021) simulated a continuous 90-day, commercialscale discharge using a TELEMAC-3D model in a hydrostatic formulation of the momentum equations. Sediment was modeled as a concentration field with a constant, unique settling velocity of  $0.1 \text{ mm s}^{-1}$  based on field observations. The model results (see Figure 4c.d) show that in the passive-transport phase the plume is narrow and meandering owing to the predominant role of advection by background currents. In the event that the magnitude of the background currents does not vary significantly, the extent of the return plume achieves a quasi-steady state; i.e., changes in current heading primarily serve to change the direction of transport but not the extent of the plume. Potentially key plume metrics such as the volume occupied by the plume, its maximum horizontal extent, and its maximum depth are greatly influenced by the choice of dilution factor (or concentration threshold), and for a given dilution factor these metrics are not continuously increasing in time due to dilution by turbulent diffusion and vertical stretching by differential settling.

A key consideration is that fluid within the often-depicted contours of dilution (e.g., Figure 4c,d) is continuously being replaced by new fluid and particles. Thus, the amount of fluid to ever exceed a threshold concentration (or to be below a desired dilution factor) is best determined as a volume flux integrated over time. While the instantaneous volume of fluid above a threshold may reach a quasi-steady state in slow-varying conditions, the total volume of fluid to have ever exceeded the threshold is a monotonically increasing function of time. In order to gain insight into how such extent metrics vary with key operational and physical oceanography parameters, Ouillon et al. (2022a) considered a simplified advection-diffusion-settling model of midwater return plumes in a steady state. Unlike for the collector plume, the extent of return plumes was found to depend most strongly, and in equal and opposed ways, on the amount of sediment being discharged and on the concentration threshold considered, confirming the observations of Muñoz-Royo et al. (2021). They found that for the long-settling timescales associated with a midwater return plume, differential settling resulting from polydispersity plays a crucial role in settling the extent of the plume, in particular in the vertical direction (Ouillon et al. 2022a). This is primarily because the vertical turbulent diffusion length scale increases with the square root of time, whereas the vertical stretching induced by differential settling increases linearly with time and is proportional on first order to the range of particle-settling velocities; thus, on a sufficiently long timescale, differential settling will overcome diffusion. Indeed, in the stratified midwater column, vertical turbulent mixing is very weak, with typical vertical turbulent diffusivities on the order of 10<sup>-6</sup>-10<sup>-4</sup> m<sup>2</sup> s<sup>-1</sup> (Waterhouse et al. 2014, Cyriac et al. 2021), and so the vertical extent of the return plume quickly becomes driven by settling, not turbulent mixing. Interestingly, an increase in both the particle-settling velocity and differential settling leads to an increase in the maximum depth reached by the plume but reductions in both the horizontal reach from the source and the instantaneous volume of fluid above the concentration threshold.

The key role played by polydispersity and the resulting differential settling on setting the extent of midwater return plumes (Ouillon et al. 2022a) mandates that models account for polydispersity. In an Eulerian approach in which the particle velocity distribution is discretized into a finite number of particle-settling velocities and in the presence of very weak vertical diffusion, the number of particle-settling velocities considered needs to be great enough that the plume does not form nonphysical, discontinuous streaks. For instance, assuming that  $\kappa_z \sim 10^{-5}~\text{m}^2~\text{s}^{-1}$  and that the model discretizes the particle velocity distribution with a resolution of 0.1 mm s<sup>-1</sup>, then the center of mass of two neighbor plumes (by the term neighbor we mean the closest plume in terms of the settling velocity) after 10 days will be separated by a vertical distance of over 80 m, while turbulent diffusion will have, over the same timescale, diffused the plumes over a vertical distance on the order of 6 m. Thus, the combination of weak vertical turbulent diffusion and long simulation timescales means that the particle-settling velocity distribution needs to be discretized with great resolution, increasing the computational cost markedly. An alternative solution might be to add a term to the advection-diffusion-settling equation that models differential settling in such a way that a coarser discretization of the particle velocity distribution remains acceptable. We note also that Lagrangian approaches used for collector plumes (Aleynik et al. 2017, Spearman et al. 2020) may be better suited to cope with the issue of differential settling. These methods typically rely on a random-walk approach to model turbulent diffusion, however, that requires that large numbers of particles be considered. It follows that if many settling velocities need to be considered, and each settling velocity requires a large number of Lagrangian particles to accurately represent turbulent diffusion, then Lagrangian approaches might suffer from similar increases in computational cost. A consensus on how best to model sediment transport in midwater return plumes has yet to be reached, and hybrid Lagrangian approaches that address such issues should be considered and developed.

#### 2.4. Seafloor Massive Sulfide and Cobalt Crust Mining Plumes

Given that the majority of known SMS deposits are connected to ocean ridges and island arc systems (Cherkashov 2017), and that cobalt crusts form on the flanks of seamounts (Usui & Suzuki 2022), the physical oceanography for these settings is markedly different from that of nodule mining (**Figure 1**). Generally, seafloor ridges and seamounts present rough seafloor and sharply defined topographical features that are associated with strong internal tides and relatively high levels of turbulence (Voet et al. 2016; van Haren 2017, 2019). Current velocities, as a result of the interaction of tides, topography, and stratification, can be O(10) cm s<sup>-1</sup> (Thurnherr et al. 2002, 2005), with high levels of variability around the mean flow (Lahaye et al. 2019). In the rift valley of the Mid-Atlantic Ridge south of the Azores, for example, mean flows on the order of 2–8 cm s<sup>-1</sup> were found over 46 days at two different locations in the valley, with maxima of 14–24 cm s<sup>-1</sup> (Keller et al. 1975). Combined with the transient nature of internal wave breaking and turbulence, this makes the physical oceanography of SMS and cobalt crust mining operations more complex and more dynamic than that of nodule mining. To date, there has been only one modeling study of an SMS sediment plume scenario (Spearman et al. 2020), which highlighted the strong influence of quickly varying background currents on sediment transport.

In addition to influencing the physical oceanography, the topography associated with SMS and cobalt crust mining has the potential to substantially affect the buoyancy-driven phase of the collector plume in the event that a turbidity current is generated. The propagation of down- and upslope gravity and turbidity currents has been studied in some detail for the canonical lock-release configuration (Bonnecaze & Lister 1999, Maxworthy 2010, Negretti et al. 2017). The ability of downslope turbidity currents to autosuspend, and therefore propagate over very long distances, is a complex open question that involves slope and geometric confinement (Wells & Dorrell 2021). Downslope propagation into a stratified ambient also leads to complex intrusion behaviors, resulting in the plume lifting off of the slope and intruding horizontally at a point of neutral buoyancy (Snow & Sutherland 2014, Ouillon et al. 2019), potentially creating secondary passively transported plumes, as depicted in **Figure 1***d* for cobalt crust mining.

The complexity of SMS and cobalt crust mining collector plumes suggests that any modeling effort to predict their evolution and extent needs to be highly location and time specific, as well as being informed by in situ measurement of ocean conditions, currents, turbulence levels, stratification, and topography. A single model is unlikely to be able to capture all the relevant physics of the plume, from discharge to far-field transport, and a multiphysics, multiscale approach should be adopted that resolves the near-field processes that control the discharge. Approaches to solve the far-field evolution of mining plumes that make broad assumptions about the sediment distribution following the discharge and buoyancy-driven phases are not well-suited to benthic SMS and cobalt crust mining sediment plumes. While little guidance currently exists for the cobalt crust scenario, natural plumes from hydrothermal vents (black smokers) have been studied in some detail (see, e.g., Klinkhammer & Hudson 1986, Konn et al. 2016). While there are key differences between hydrothermal plumes and SMS mining sediment plumes (most notably the opposite sign of the plume's buoyancy), much can likely be learned from hydrothermal plume data, particularly from existing data on the extent of such plumes in the passive-transport phase.

#### 3. FURTHER CONSIDERATIONS

The fluid mechanics of deep-sea mining extends beyond sediment plumes into the arenas of sediment settling and rheology as well as the design and operation of mining systems. In this section, we highlight some of the other key open research questions for the fluid mechanics community.

#### 3.1. Sediment Properties

A key issue for the modeling of sediment plumes is the adequate representation of particle settling, which depends on the size and shape of individual particles but also on the flocculation of sediment into larger, porous flocs, the settling velocity of which markedly differs from disaggregated sediment. Gillard et al. (2019) conducted laboratory experiments on the flocculation properties of sediment from the CCZ, through both differential settling (zero shear) and inertial processes (turbulent shear). For relatively high sediment mass concentrations ( $\sim$ 500 mg L<sup>-1</sup>) and shear rates ( $\sim 10 \text{ s}^{-1}$ ), the researchers found that rapid flocculation occurred within 10 min. This suggests that nodule collector plume modeling efforts should pay close attention to the role played by flocculation in setting the initial conditions for the sediment particle size distribution and settling velocity distribution. Furthermore, any other process that affects sediment transport in the initial phases after discharge, when the plume is still highly concentrated, may affect flocculation. In collector plumes, for instance, the turbidity current regime generated by the plume's negative buoyancy after discharge may lead to different flocculation processes, including disaggregation. To our knowledge, flocculation processes and their role in the propagation, deposition, entrainment, and detrainment of turbidity currents have yet to be investigated. In midwater discharges, it was shown that following rapid dilution during the buoyancy-driven phase, the plume became passively advected and remained vertically consistent with a dye tracer over several hours, suggesting that flocculation played little to no role in affecting the particle size distribution and particle-settling velocity distribution for these timescales and beyond (Muñoz-Royo et al. 2021). It follows that the role of flocculation in setting the properties of the sediment and its ability to settle to the seabed may play a role in certain plume scenarios (i.e., discharge and buoyancy-driven phases for a collector plume) and not others (i.e., midwater return plume). In situ measurement techniques will therefore be essential to assess sediment properties in the various phases of the evolution of plumes (see, for instance, Gillard et al. 2022).

The rheology of the highly fluidized top layer of sediment on abyssal plains has received very little attention, yet it may play a crucial role in several plume-related transport processes. First, resuspension processes are strongly affected by the rheology of the consolidated top layer, which profoundly influences the ability of the collector plume turbidity current to erode the seabed and enter a self-accelerated regime (Wells & Dorrell 2021). Self-accelerated turbidity currents in other geophysical contexts are known to spread over very large distances and could increase the total amount of sediment resuspended by deep-sea mining beyond that picked up by a collector. Similarly, processes such as the maneuvering of collector vehicles and the ability of flow structures created by seabed operations to resuspend sediment depend markedly on the rheology of the seabed. Finally, knowing that heavy sediment redeposition occurs over distances up to tens of meters on either side of collector tracks (Burns 1980), the properties of the top layer of freshly deposited sediment are likely to be very different from those of the natural sediment coverage, and it is not currently known to what extent this sediment is more prone to resuspension. Benthic storms and periods of elevated background currents near the seabed produced by remotely generated eddies (Kontar & Sokov 1994, Aleynik et al. 2017) may also play important roles in mobilizing and resuspending freshly deposited sediment, as proposed by Aleynik et al. (2017).

Finally, a fascinating question that remains is, How is it that polymetallic nodules are naturally uncovered on the seabed when their growth rate (of a millimeter per million years) is several orders of magnitude slower than the sediment deposition rate (of a millimeter per thousand years) in the abyssal ocean? But for some yet-to-be well-established process, the nodules would be buried under meters of sediment. Whether the tools to answer this question are in the hands of the fluid mechanics community remains an open question. It has been postulated that activity of fauna in and around the nodules is responsible for keeping them clear of sediment (Dutkiewicz et al. 2020),

although no evidence for the mechanisms that keep nodules uncovered is proposed or discussed. Alternatively, it has been proposed that the interaction of background currents and seafloor topography may contribute to the removal of fines from nodules (Mewes et al. 2014), which can facilitate their growth. Background currents in the range  $1-9 \, \mathrm{cm \, s^{-1}}$  were measured during the Deep Ocean Mining Environmental Study (DOMES) experiments (Hayes 1979); for centimeter-scale nodules, this corresponds to Reynolds numbers  $O(10^2-10^3)$  that could readily produce small-scale turbulent flow structures capable of mobilizing sediment from a nodule. Certainly, a study of the flow past a partially buried polymetallic nodule could be devised that investigates the ability of background currents to remove particles of certain sizes from the nodule's surface. We finally note that the so-called Brazil nut effect, a process by which large particles rise to the surface of a vibrated granular bed of smaller particles, can be enhanced in the presence of water (Clement et al. 2010), but whether this mechanism applies to polymetallic nodules has not been investigated.

#### 3.2. Mining System Design

Several aspects of the design of deep-sea mining systems revolve around fluid mechanical processes. First, the design of efficient nodule pickup mechanisms that minimize the amount of resuspended sediment, for example, will benefit from the development and optimization of fluid dynamics-based technologies. Several collector prototypes make use of the Coandă effect, i.e., the tendency of a fluid jet approaching a curved surface to remain attached to the surface (Trancossi 2011), in order to mobilize nodules, and this approach can be optimized for reduced sediment resuspension. An alternative approach to hydrodynamic pickup is mechanical pickup of nodules via a raking system, the nodules being picked up by a front-mounted rake with the goal of minimizing the amount of sediment being resuspended. For both hydrodynamic and mechanical pickup configurations, improved nodule-sediment separation within a collector vehicle through the use of flow-based technology could control the amount of sediment brought up to a surface operation vessel and thus the amount of sediment in a return plume. One example is hydrocyclone technology, whereby centrifugal force is used to separate particles of different sizes (Cilliers 2000). In addition, given that the high-Reynolds number turbulent wake of a collector vehicle plays an important role in the discharge phase of the resulting sediment plume, consideration of the overall hydrodynamic design of a collector vehicle is also to be investigated.

Collector designs that allow for above-seabed maneuvering have been proposed, relying on buoyancy control and/or vertically oriented propellers that produce thrust to compensate for the submerged weight of the collector. While such approaches may be used to reduce or eliminate the direct seabed impact, they raise the question of induced resuspension by, say, jet impingement on the top layer of seabed sediment. While there is some literature on resuspension by jet impingement in the context of deep-sea mining (Becker et al. 2001) and more recently in the context of artificial downwelling (Fan et al. 2020), much remains to be done before resuspension of sediment can be accurately and systematically predicted. A particular nodule mining approach under consideration is to deploy swarms of autonomous robots that are not in direct contact with the seabed to individually grab and remove nodules. In addition to the substantial technological challenges associated with this approach, how such swarms of robots will interact hydrodynamically with the seabed, and to what extent the flow disturbances created would interact with sediment disturbed by nodule picking operations, is unknown. Overall, claims that a particular approach is going to be markedly better at minimizing plume disturbances than other approaches will need to be underpinned by a substantive fluid mechanical analysis. Given the complexity of the fluid processes involved, it will be crucial that any proposed collector designs be tested in a realistic environment before commercial application, and that resuspension resulting from hydrodynamic interaction of the collector-induced flow with the seabed be quantified.

Little attention has yet been given to the role played by the trajectory of a mining vehicle on the form and extent of the resulting sediment plume. Nodule collectors moving at speeds O(0.1-1) m s<sup>-1</sup> can travel much faster than background currents and potentially cover distances comparable to that of plume advection during daily operations. This suggests that the collector trajectory can play a crucial role in setting the sediment transport and deposition patterns. Considerations such as the direction of background currents with respect to collector motion (e.g., aligned, opposed, or orthogonal) are particularly relevant. The timescale of operations is also a consideration: While collectors are anticipated to move at speeds that far exceed background current velocities, a collector following a compact mining pattern will have a translational velocity that is proportional to the ratio of track spacing to track length. This means that depending on the choice of mining pattern, the ratio of the characteristic advection timescale and collector motion timescale can vary greatly, leading to plume stretching, plume accumulation, or other nontrivial processes. The potential overlap of operation and plume length and timescales further complicates the development of off-the-shelf solutions for plume modeling and extent prediction. A related question is that of induced turbulence by the mining operation itself. As mining equipment is maneuvered at or immediately above the seabed, it generates momentum in the surrounding fluid that can lead to turbulence, examples being the turbulent wake behind a nodule collector (see Section 2.2.1) or turbulent jets from proposed neutrally buoyant collector systems that maneuver just above the seabed. How this induced turbulence contributes to mixing and vertical transport of sediment, and over which time and spatial scales, has not been formally assessed and will be highly dependent on the mining technology and its operation.

Riser systems are the primary means considered for vertical transport from the seabed to the surface operation vessel for all forms of seabed mining. Such risers experience vortex-induced vibrations (VIVs), which have been extensively studied and reviewed in a general fluid mechanics context (Williamson & Govardhan 2004) as well as recently in the context of marine risers (Hong & Shah 2018). Active control of VIVs is typically carried out through some top boundary control, which becomes less efficient for deep risers such as those needed for deep-sea mining. Furthermore, for nodule mining, both the top and bottom boundaries of the riser system are in motion, increasing the potential sources of VIV excitation but also the potential for active control at both boundaries. Additional complexity is added when considering temporal variability in the density of the fluid in the riser system. Indeed, Thorsen et al. (2019) argues that such variability can affect VIV of riser systems and lead to both increased and decreased fatigue. It would seem that VIVinduced fatigue failure of deep-sea mining riser systems brings new challenges that should be of interest to the VIV research community. Finally, pumping and transporting the slurry of nodules, sediment, and seawater through the riser system lead to additional challenges such as blockage (van Wijk et al. 2015) or variable performance and mechanical stress levels (Dai et al. 2021), all of which will benefit from further research.

#### **SUMMARY POINTS**

- 1. Fluid mechanics underlies a panoply of environmental and engineering challenges surrounding the nascent deep-sea mining industry.
- 2. Research into sediment plume transport, which is central to the issue of the extent of environmental impact, must rely on an appropriate combination of laboratory experiments, theory, multiscale numerical modeling, and, crucially, field studies.
- 3. The evolution of sediment plumes typically involves three phases: the discharge phase, the buoyancy-driven phase, and the passive-transport phase.

- 4. Negative buoyancy induced by sediment loading drives turbidity currents in the buoyancy-driven phase, which are further influenced by multiple environmental factors (e.g., slope, background currents, and sediment rheology), with critical implications for the fate of suspended sediment in the passive-transport phase.
- Advection, turbulent diffusion, and dispersion associated with the background physical oceanography, combined with sediment settling, control the passive transport of sediment plumes.
- Different metrics can be used to assess the extent of sediment plume disturbances, which often vary nonlinearly with the key parameters.

#### **FUTURE ISSUES**

- The active engagement and scientific leadership of the fluid mechanics research community are vital to underpin informed decision-making by international governance and contractors as well as, more broadly, to inform society regarding the nascent deep-sea mining industry.
- Numerical modeling of sediment plumes faces inherent challenges that need to be properly addressed to produce reliable predictions that will be central to decision-making processes.
- In situ measurements of background physical oceanography, particularly turbulence, and of sediment properties, in combination with in situ data from technology field trials, will be critical for making realistic model predictions of plumes.
- 4. For all forms of deep-sea mining, establishing the overall sediment budget (i.e., mobilized sediment, local deposition, and passive transport by background currents) will be key, with additional sediment mobilized by turbidity currents potentially an important consideration.
- 5. Research is more advanced for polymetallic nodule mining than for seafloor massive sulfide and cobalt crust mining, but in all cases the future design and operation of proposed mining technology are in pressing need of fundamental fluid mechanics insight.
- The development of plume extent metrics must be guided by the needs of the broader community, in particular the deep-sea ecology scientific community.

#### **DISCLOSURE STATEMENT**

The authors are not aware of any biases that might be perceived as affecting the objectivity of this review.

#### ACKNOWLEDGMENTS

The authors acknowledge the support of the Massachusetts Institute of Technology Environmental Solutions Initiative, the Office of Naval Research, the 11th Hour Project of the Schmidt Family Foundation, the Benioff Ocean Initiative (the funders had no role in any aspects of the research), and the National Science Foundation (through CBET grant 2139277). Furthermore, we extend thanks to Matthew Alford and Carlos Muñoz Royo for their assistance in preparing the manuscript and to Glynn Gorick for the preparation of **Figures 1**, **2**, and **5**.

#### LITERATURE CITED

- Aleynik D, Inall ME, Dale A, Vink A. 2017. Impact of remotely generated eddies on plume dispersion at abyssal mining sites in the Pacific. Sci. Rep. 7(1):16959
- Alford MH, MacKinnon JA, Simmons HL, Nash JD. 2016. Near-inertial internal gravity waves in the ocean. Annu. Rev. Mar. Sci. 8:95–123
- Baker ET, Massoth GJ. 1986. Hydrothermal plume measurements: a regional perspective. Science 234(4779):980–82
- Becker HJ, Grupe B, Oebius HU, Liu F. 2001. The behaviour of deep-sea sediments under the impact of nodule mining processes. *Deep Sea Res. Part II Top. Stud. Oceanogr.* 48(17–18):3609–27
- Blanchette F, Strauss M, Meiburg E, Kneller B, Glinsky ME. 2005. High-resolution numerical simulations of resuspending gravity currents: conditions for self-sustainment. *J. Geophys. Res.* 110(C12):C12022
- Bonnecaze RT, Lister JR. 1999. Particle-driven gravity currents down planar slopes. J. Fluid Mech. 390:75-91
- Burns RE. 1980. Assessment of environmental effects of deep ocean mining of manganese nodules. Helgol. Meeresunters. 33(1–4):433–42
- Cherkashov G. 2017. Seafloor massive sulfide deposits: distribution and prospecting. In *Deep-Sea Mining*, ed. R Sharma, pp. 143–64. Cham, Switz.: Springer Int.
- Chowdhury MR, Testik FY. 2015. Axisymmetric underflows from impinging buoyant jets of dense cohesive particle-laden fluids. J. Hydraul. Eng. 141(3):04014079
- Cilliers J. 2000. Particle size separation. Hydrocyclones for particle size separation. In Encyclopedia of Separation Science, pp. 1819–25. San Diego, CA: Academic Press
- Clement CP, Pacheco-Martinez HA, Swift MR, King PJ. 2010. The water-enhanced Brazil nut effect. Europhys. Lett. 91(5):54001
- Concha AF. 2014. Particle aggregation by coagulation and flocculation. In Solid–Liquid Separation in the Mining Industry, pp. 143–72. Cham, Switz.: Springer
- Cyriac A, Phillips HE, Bindoff NL, Mao H, Feng M. 2021. Observational estimates of turbulent mixing in the southeast Indian Ocean. J. Phys. Oceanogr. 51(7):2103–28
- Dai Y, Zhang Y, Li X. 2021. Numerical and experimental investigations on pipeline internal solid-liquid mixed fluid for deep ocean mining. *Ocean Eng.* 220:108411
- Derakhshandeh JF, Alam MM. 2019. A review of bluff body wakes. Ocean Eng. 182:475-88
- Derjaguin BV, Churaev NV, Muller VM. 1987. The Derjaguin–Landau–Verwey–Overbeek (DLVO) theory of stability of lyophobic colloids. In *Surface Forces*, ed. NV Churaev, BV Derjaguin, VM Muller, pp. 293–310. Boston, MA: Springer
- Devenish BJ, Rooney GG, Webster HN, Thomson DJ. 2010. The entrainment rate for buoyant plumes in a crossflow. *Bound.-Layer Meteorol.* 134(3):411–39
- Devkota BH, Imberger J. 2009. Lagrangian modeling of advection-diffusion transport in open channel flow. Water Resour. Res. 45(12):W12406
- Dorrell RM, Hogg AJ, Pritchard D. 2013. Polydisperse suspensions: erosion, deposition, and flow capacity. 7. Geophys. Res. Earth Surf. 118(3):1939–55
- Dorrell RM, Hogg AJ, Sumner EJ, Talling PJ. 2011. The structure of the deposit produced by sedimentation of polydisperse suspensions. J. Geophys. Res. Earth Surf. 116:F01024
- Dorrell RM, Peakall J, Darby SE, Parsons DR, Johnson J, et al. 2019. Self-sharpening induces jet-like structure in seafloor gravity currents. *Nat. Commun.* 10:1381
- Dutkiewicz A, Judge A, Müller RD. 2020. Environmental predictors of deep-sea polymetallic nodule occurrence in the global ocean. Geology 48(3):293–97
- Elerian M, Alhaddad S, Helmons R, van Rhee C. 2021. Near-field analysis of turbidity flows generated by polymetallic nodule mining tools. *Mining* 1(3):251–78
- Ernst GGJ, Sparks RSJ, Carey SN, Bursik MI. 1996. Sedimentation from turbulent jets and plumes. J. Geophys. Res. 101(B3):5575–89
- Fan W, Bao W, Cai Y, Xiao C, Zhang Z, et al. 2020. Experimental study on the effects of a vertical jet impinging on soft bottom sediments. *Sustainability* 12(9):3775
- Gardner WD, Richardson MJ, Mishonov AV, Biscaye PE. 2018. Global comparison of benthic nepheloid layers based on 52 years of nephelometer and transmissometer measurements. *Prog. Oceanogr*: 168:100–11

- Gillard B, Harbour RP, Nowald N, Thomsen L, Iversen MH. 2022. Vertical distribution of particulate matter in the Clarion Clipperton Zone (German sector)—potential impacts from deep-sea mining discharge in the water column. Front. Mar. Sci. 9:820947
- Gillard B, Purkiani K, Chatzievangelou D, Vink A, Iversen MH, Thomsen L. 2019. Physical and hydrodynamic properties of deep sea mining-generated, abyssal sediment plumes in the Clarion Clipperton Fracture Zone (eastern-central Pacific). Elementa 7:5
- Gladstone C, Phillips JC, Sparks RSJ. 1998. Experiments on bidisperse, constant-volume gravity currents: propagation and sediment deposition. *Sedimentology* 45(5):833–43
- Hage S, Cartigny MJ, Sumner EJ, Clare MA, Hughes Clarke JE, et al. 2019. Direct monitoring reveals initiation of turbidity currents from extremely dilute river plumes. Geophys. Res. Lett. 46(20):11310–20
- Hallworth MA, Hogg AJ, Huppert HE. 1998. Effects of external flow on compositional and particle gravity currents. 7. Fluid Mech. 359:109–42
- Hallworth MA, Huppert HE, Phillips JC, Sparks RSJ. 1996. Entrainment into two-dimensional and axisymmetric turbulent gravity currents. *7. Fluid Mech.* 308:289–311
- Hallworth MA, Phillips JC, Huppert HE, Sparks RSJ. 1993. Entrainment in turbulent gravity currents. *Nature* 362(6423):829–31
- Harris TC, Hogg AJ, Huppert HE. 2002. Polydisperse particle-driven gravity currents. *J. Fluid Mech.* 472:333–71
- Hayes SP. 1979. Benthic current observations at DOMES sites A, B, and C in the tropical North Pacific Ocean. In *Marine Geology and Oceanography of the Pacific Manganese Nodule Province*, ed. JL Bischoff, DZ Piper, pp. 83–112. Boston, MA: Springer
- Hein JR, Koschinsky A, Kuhn T. 2020. Deep-ocean polymetallic nodules as a resource for critical materials. Nat. Rev. Earth Environ. 1(3):158–69
- Hong K-S, Shah UH. 2018. Vortex-induced vibrations and control of marine risers: a review. Ocean Eng. 152:300–15
- Howell J. 2011. The decay of bluff body wakes. SAE Int. J. Passeng. Cars Mech. Syst. 4(1):207–15
- James CB, Mingotti N, Woods AW. 2022. On particle separation from turbulent particle plumes in a crossflow. J. Fluid Mech. 932:A45
- Jankowski J, Malcherek A, Zielke W. 1994. Numerical modeling of sediment transport processes caused by deep sea mining discharges. In *Proceedings of OCEANS'94*, Vol. 3, pp. 269–77. New York: IEEE
- Jankowski JA, Malcherek A, Zielke W. 1996. Numerical modeling of suspended sediment due to deep-sea mining. J. Geophys. Res. Oceans 101(C2):3545–60
- Jankowski JA, Zielke W. 2001. The mesoscale sediment transport due to technical activities in the deep sea. Deep Sea Res. Part II Top. Stud. Oceanogr. 48(17–18):3487–521
- Jones DO, Simon-Lledó E, Amon DJ, Bett BJ, Caulle C, et al. 2021. Environment, ecology, and potential effectiveness of an area protected from deep-sea mining (Clarion Clipperton Zone, abyssal Pacific). Prog. Oceanogr. 197:102653
- Keller GH, Anderson SH, Lavelle JW. 1975. Near-bottom currents in the Mid-Atlantic Ridge rift valley. Can. 7. Earth Sci. 12(4):703–10
- Klinkhammer G, Hudson A. 1986. Dispersal patterns for hydrothermal plumes in the South Pacific using manganese as a tracer. *Earth Planet. Sci. Lett.* 79(3–4):241–49
- Kneller B, Nasr-Azadani MM, Radhakrishnan S, Meiburg E. 2016. Long-range sediment transport in the world's oceans by stably stratified turbidity currents. J. Geophys. Res. Oceans 121(12):8608–20
- Konn C, Fourré E, Jean-Baptiste P, Donval JP, Guyader V, et al. 2016. Extensive hydrothermal activity revealed by multi-tracer survey in the Wallis and Futuna region (SW Pacific). Deep Sea Res. Part I Oceanogr. Res. Pap. 116:127–44
- Kontar EA, Sokov AV. 1994. A benthic storm in the northeastern tropical Pacific over the fields of manganese nodules. Deep Sea Res. Part I Oceanogr. Res. Pap. 41(7):1069–89
- Lahaye N, Gula J, Thurnherr AM, Reverdin G, Bouruet-Aubertot P, Roullet G. 2019. Deep currents in the rift valley of the North Mid-Atlantic Ridge. Front. Mar. Sci. 6:597
- Lavelle JW, Ozturgut E, Swift SA, Erickson BH. 1981. Dispersal and resedimentation of the benthic plume from deep-sea mining operations: a model with calibration. *Mar. Min.* 3(1–2):59–93

- Lee JH-W, Chu VH. 2003. Turbulent Tets and Plumes. Boston, MA: Springer
- Lermusiaux PFJ, Schröter J, Danilov S, Iskandarani M, Pinardi N, Westerink JJ. 2013. Multiscale modeling of coastal, shelf, and global ocean dynamics. *Ocean Dyn.* 63(11–12):1341–44
- List EJ. 1982. Turbulent jets and plumes. Annu. Rev. Fluid Mech. 14:189-212
- Luchi R, Balachandar S, Seminara G, Parker G. 2018. Turbidity currents with equilibrium basal driving layers: a mechanism for long runout. Geophys. Res. Lett. 45(3):1518–26
- Maxworthy T. 2010. Experiments on gravity currents propagating down slopes. Part 2. The evolution of a fixed volume of fluid released from closed locks into a long, open channel. *J. Fluid Mecb.* 647:27–51
- Maxworthy T, Leilich J, Simpson JE, Meiburg E. 2002. The propagation of a gravity current into a linearly stratified fluid. 7. Fluid Mech. 453:371–94
- Meiburg E, Kneller B. 2010. Turbidity currents and their deposits. Annu. Rev. Fluid Mech. 42:135-56
- Mewes K, Mogollón JM, Picard A, Rühlemann C, Kuhn T, et al. 2014. Impact of depositional and biogeochemical processes on small scale variations in nodule abundance in the Clarion-Clipperton Fracture Zone. Deep Sea Res. Part I Oceanogr. Res. Pap. 91:125–41
- Mingotti N, Woods AW. 2020. Stokes settling and particle-laden plumes: implications for deep-sea mining and volcanic eruption plumes. Philos. Trans. R. Soc. A Math. Phys. Eng. Sci. 378(2179):20190532
- Morton BR, Taylor G, Turner J. 1956. Turbulent gravitational convection from maintained and instantaneous sources. *Proc. R. Soc. A Math. Phys. Sci.* 234(1196):1–23
- Muñoz-Royo C, Ouillon R, El Mousadik S, Alford MH, Peacock T. 2022. An in-situ study of turbidity-current plumes generated by a prototype deep-sea nodule mining vehicle. *Sci. Adv.* 8(38):eabn1219
- Muñoz-Royo C, Peacock T, Alford MH, Smith JA, Le Boyer A, et al. 2021. Extent of impact of deep-sea nodule mining midwater plumes is influenced by sediment loading, turbulence and thresholds. Commun. Earth Environ. 2:148
- Necker F, Härtel C, Kleiser L, Meiburg E. 2005. Mixing and dissipation in particle-driven gravity currents. 7. Fluid Mech. 545:339–72
- Negretti ME, Flor JB, Hopfinger EJ. 2017. Development of gravity currents on rapidly changing slopes. *J. Fluid Mecb.* 833:70–97
- Nojiri Y, Ishibashi J, Kawai T, Otsuki A, Sakai H. 1989. Hydrothermal plumes along the North Fiji Basin spreading axis. Nature 342:667–70
- Oebius HU, Becker HJ, Rolinski S, Jankowski JA. 2001. Parametrization and evaluation of marine environmental impacts produced by deep-sea manganese nodule mining. Deep Sea Res. Part II Top. Stud. Oceanogr. 48(17–18):3453–67
- Ouillon R, Kakoutas C, Meiburg E, Peacock T. 2021. Gravity currents from moving sources. J. Fluid Mech. 924:A43
- Ouillon R, Meiburg E, Sutherland BR. 2019. Turbidity currents propagating down a slope into a stratified saline ambient fluid. Environ. Fluid Mech. 19:1143–66
- Ouillon R, Muñoz-Royo C, Alford MH, Peacock T. 2022a. Advection-diffusion-settling of deep-sea mining sediment plumes. Part I: Midwater plumes. Flow 2:E22
- Ouillon R, Muñoz-Royo C, Alford MH, Peacock T. 2022b. Advection-diffusion-settling of deep-sea mining sediment plumes. Part II: Collector plumes. Flow 2:E23
- Peacock T, Alford MH. 2018. Is deep-sea mining worth it? Sci. Am. 318(5):72-77
- Purkiani K, Gillard B, Paul A, Haeckel M, Haalboom S, et al. 2021. Numerical simulation of deep-sea sediment transport induced by a dredge experiment in the northeastern Pacific Ocean. Front. Mar. Sci. 8:719463
- Purkiani K, Paul A, Vink A, Walter M, Schulz M, Haeckel M. 2020. Evidence of eddy-related deep-ocean current variability in the northeast tropical Pacific Ocean induced by remote gap winds. *Biogeosciences* 17(24):6527–44
- Resing JA, Sedwick PN, German CR, Jenkins WJ, Moffett JW, et al. 2015. Basin-scale transport of hydrothermal dissolved metals across the South Pacific Ocean. *Nature* 523(7559):200–3
- Richardson MJ, Weatherly GL, Gardner WD. 1993. Benthic storms in the Argentine Basin. *Deep Sea Res. Part II Top. Stud. Oceanogr.* 40(4–5):975–87
- Rolinski S, Segschneider J, Sündermann J. 2001. Long-term propagation of tailings from deep-sea mining under variable conditions by means of numerical simulations. *Deep Sea Res. Part II Top. Stud. Oceanogr*. 48(17–18):3469–85

- Rzeznik AJ, Flierl GR, Peacock T. 2019. Model investigations of discharge plumes generated by deep-sea nodule mining operations. *Ocean Eng.* 172:684–96
- Segschneider J, Sündermann J. 1998. Simulating large scale transport of suspended matter. J. Mar. Syst. 14(1–2):81–97
- Sharma R. 2017. Deep-Sea Mining. Cham, Switz.: Springer Int.
- Smith CR, Tunnicliffe V, Colaço A, Drazen JC, Gollner S, et al. 2020. Deep-sea misconceptions cause underestimation of seabed-mining impacts. *Trends Ecol. Evol.* 35(10):853–57
- Snow K, Sutherland BR. 2014. Particle-laden flow down a slope in uniform stratification. J. Fluid Mech. 755:251–73
- Sparks RSJ. 1986. The dimensions and dynamics of volcanic eruption columns. Bull. Volcanol. 48:3-15
- Spearman J, Taylor J, Crossouard N, Cooper A, Turnbull M, et al. 2020. Measurement and modelling of deep sea sediment plumes and implications for deep sea mining. Sci. Rep. 10:5075
- Thorsen M, Challabotla N, Sævik S, Nydal O. 2019. A numerical study on vortex-induced vibrations and the effect of slurry density variations on fatigue of ocean mining risers. *Ocean Eng.* 174:1–13
- Thurnherr AM, Richards KJ, German CR, Lane-Serff GF, Speer KG. 2002. Flow and mixing in the rift valley of the Mid-Atlantic Ridge. 7. Phys. Oceanogr. 32(6):1763–78
- Thurnherr AM, St. Laurent LC, Speer KG, Toole JM, Ledwell JR. 2005. Mixing associated with sills in a canyon on the midocean ridge flank. 7. Phys. Oceanogr. 35(8):1370-81
- Trancossi M. 2011. An overview of scientific and technical literature on Coanda effect applied to nozzles. SAE Tech. Pap. 2011-01-2591, SAE Int., Warrandale, PA
- Usui A, Suzuki K. 2022. Geological characterization of ferromanganese crust deposits in the NW Pacific seamounts for prudent deep-sea mining. In *Perspectives on Deep-Sea Mining*, ed. R Sharma, pp. 81–113. Cham, Switz.: Springer Int.
- van der Grient J, Drazen J. 2021. Potential spatial intersection between high-seas fisheries and deep-sea mining in international waters. *Mar. Policy* 129:104564
- van Haren H. 2017. Exploring the vertical extent of breaking internal wave turbulence above deep-sea topography. *Dyn. Atmos. Oceans* 77:89–99
- van Haren H. 2018. Abyssal plain hills and internal wave turbulence. Biogeosciences 15(14):4387-403
- van Haren H. 2019. Off-bottom turbulence expansions of unbounded flow over a deep-ocean ridge. *Tellus A Dyn. Meteorol. Oceanogr.* 71(1):1653137
- van Wijk JM, van Grunsven F, Talmon AM, van Rhee C. 2015. Simulation and experimental proof of plug formation and riser blockage during vertical hydraulic transport. *Ocean Eng.* 101:58–66
- Voet G, Alford MH, Girton JB, Carter GS, Mickett JB, Klymak JM. 2016. Warming and weakening of the abyssal flow through Samoan Passage. J. Phys. Oceanogr. 46(8):2389–401
- Wang D, Adams EE. 2021. Secondary intrusion formation of multiphase plumes. Front. Mar. Sci. 8:61707
- Waterhouse AF, MacKinnon JA, Nash JD, Alford MH, Kunze E, et al. 2014. Global patterns of diapycnal mixing from measurements of the turbulent dissipation rate. J. Phys. Oceanogr. 44(7):1854–72
- Weaver P, Aguzzi J, Boschen-Rose R, Colaço A, de Stigter H, et al. 2022. Assessing plume impacts caused by polymetallic nodule mining vehicles. Mar. Policy 139:105011
- Wells M, Dorrell R. 2021. Turbulence processes within turbidity currents. Annu. Rev. Fluid Mech. 53:59-83
- Williamson C, Govardhan R. 2004. Vortex-induced vibrations. Annu. Rev. Fluid Mech. 36:413-55
- Woods AW. 2010. Turbulent plumes in nature. Annu. Rev. Fluid Mech. 42:391-412
- Yeh GT. 1990. A Lagrangian-Eulerian Method with zoomable hidden fine-mesh approach to solving advection-dispersion equations. Water Resour. Res. 26(6):1133–44
- Zhao K, Pomes F, Vowinckel B, Hsu TJ, Bai B, Meiburg E. 2021. Flocculation of suspended cohesive particles in homogeneous isotropic turbulence. J. Fluid Mech. 921:A17



# Annual Review of Fluid Mechanics

Volume 55, 2023

# Contents

1
11
45
77
103
129
157
193
213
237
265
291

Gas-Liquid Foam Dynamics: From Structural Elements to Continuum  Descriptions  Peter S. Stewart and Sascha Hilgenfeldt	23
Recent Developments in Theories of Inhomogeneous and Anisotropic Turbulence  J.B. Marston and S.M. Tobias 3	51
Icebergs Melting Claudia Cenedese and Fiamma Straneo	77
The Fluid Mechanics of Deep-Sea Mining  Thomas Peacock and Raphael Ouillon 40	03
A Perspective on the State of Aerospace Computational Fluid Dynamics Technology Mori Mani and Andrew J. Dorgan	31
Particle Rafts and Armored Droplets Suzie Protière 4:	59
Evaporation of Sessile Droplets Stephen K. Wilson and Hannah-May D'Ambrosio	81
3D Lagrangian Particle Tracking in Fluid Mechanics  Andreas Schröder and Daniel Schanz	11
Linear Flow Analysis Inspired by Mathematical Methods from Quantum Mechanics Luca Magri, Peter J. Schmid, and Jonas P. Moeck	41
Transition to Turbulence in Pipe Flow  Marc Avila, Dwight Barkley, and Björn Hof	75
Turbulent Rotating Rayleigh–Bénard Convection  Robert E. Ecke and Olga Shishkina	03
Nonidealities in Rotating Detonation Engines  Venkat Raman, Supraj Prakash, and Mirko Gamba	39
Elasto-Inertial Turbulence  Yves Dubief, Vincent E. Terrapon, and Björn Hof	75
Sharp Interface Methods for Simulation and Analysis of Free Surface Flows with Singularities: Breakup and Coalescence Christopher R. Anthony, Hansol Wee, Vishrut Garg, Sumeet S. Thete, Pritish M. Kamat, Brayden W. Wagoner, Edward D. Wilkes, Patrick K. Notz, Alvin U. Chen, Ronald Suryo, Krishnaraj Sambath, Jayanta C. Panditaratne, Ying-Chih Liao, and Osman A. Basaran	07

### **Indexes**

Cumulative Index of Contributing Authors, Volumes 1–55	749
Cumulative Index of Article Titles, Volumes 1–55	760

### Errata

An online log of corrections to Annual Review of Fluid Mechanics articles may be found at http://www.annualreviews.org/errata/fluid